27. Lanford, P. J., Lan, Y., Jiang, R., Lindsell, C., Weinmaster, G., Gridley, T. & Kelley, M. W. *Nat Genet* **21**, 289-92 (1999).
28. Woods, C., Montcouquiol, M. & Kelley, M. W. *Nat Neurosci* (2004).
29. Kanzaki, S., Kawamoto, K., Oh, S. H., Stover, T., Suzuki, M., Ishimoto, S., Yagi, M., Miller, J. M., Lomax, M. I. & Raphael, Y. *Audiol Neurootol* 7, 161-4 (2002).
30. Zheng, J. L., Helbig, C. & Gao, W. Q. *J Neurosci* **17**, 216-26 (1997).
31. Yamashita, H. & Oesterle, E. C. *Proc Natl Acad Sci U S A* **92**, 3152-5 (1995).
32. Kuntz, A. L. & Oesterle, E. C. *J Comp Neurol* **399**, 413-23 (1998).
33. Chen, P. & Segil, N. *Development* **126**, 1581-90 (1999).
34. Cheng, M., Olivier, P., Diehl, J. A., Fero, M., Roussel, M. F., Roberts, J. M. & Sherr, C. J. *Embo J* **18**, 1571-83 (1999).
35. Lowenheim, H., Furness, D. N., Kil, J., Zinn, C., Gultig, K., Fero, M. L., Frost, D., Gummer, A. W., Roberts, J. M., Rubel, E. W., Hackney, C. M. & Zenner, H. P. *Proc Natl Acad Sci U S A* **96**, 4084-8 (1999).
36. Morrison, A., Hodgetts, C., Gossler, A., Hrabe de Angelis, M. & Lewis, J. *Mech Dev* **84**, 169-72 (1999).
37. Zheng, J. L. & Gao, W. Q. *Nat Neurosci* **3**, 580-6 (2000).
38. Shou, J., Zheng, J. L. & Gao, W. Q. *Mol Cell Neurosci* **23**, 169-79 (2003).
39. Zine, A., Aubert, A., Qiu, J., Therianos, S., Guillemot, F., Kageyama, R. & de Ribaupierre, F. *J Neurosci* **21**, 4712-20 (2001).
40. Li, H., Liu, H. & Heller, S. *Nat Med* **9**, 1293-9 (2003).
41. Yamaguchi, M., Saito, H., Suzuki, M. & Mori, K. *Neuroreport* **11**, 1991-6 (2000).
42. Kawaguchi, A., Miyata, T., Sawamoto, K., Takashita, N., Murayama, A., Akamatsu, W., Ogawa, M., Okabe, M., Tano, Y., Goldman, S. A. & Okano, H. *Mol Cell Neurosci* **17**, 259-73 (2001).
43. Kojima, K., Takebayashi, S., Nakagawa, T., Iwai, K. & Ito, J. *Acta Otolaryngol Suppl*, 14-7 (2004).
44. Lopez, I. A., Zhao, P. M., Yamaguchi, M., de Vellis, J. & Espinosa-Jeffrey, A. *Int J Dev Neurosci* **22**, 205-13 (2004).
45. Drucker-Colin, R. & Verdugo-Diaz, L. *Cell Mol Neurobiol* **24**, 301-16 (2004).
46. Duggal, N., Schmidt-Kastner, R. & Hakim, A. M. *Brain Res* **768**, 1-9 (1997).
47. Ito, J., Kojima, K. & Kawaguchi, S. *Acta Otolaryngol* **121**, 140-2 (2001).
48. Naito, Y., Nakamura, T., Nakagawa, T., Iguchi, F., Endo, T., Fujino, K., Kim, T. S., Hiratsuka, Y., Tamura, T., Kanemaru, S., Shimizu, Y. & Ito, J. *Neuroreport* **15**, 1-4 (2004).
49. Kojima, K., Murata, M., Nishio, T., Kawaguchi, S. & Ito, J. *Acta Otolaryngol Suppl*, 53-5 (2004).
50. Kohyama, J., Abe, H., Shimazaki, T., Koizumi, A., Nakashima, K., Gojo, S., Taga, T., Okano, H., Hata, J. & Umezawa, A. *Differentiation* **68**, 235-44 (2001).
51. Lindvall, O., Kokaia, Z. & Martinez-Serrano, A. *Nat Med* **10 Suppl**, S42-50 (2004).
52. Kawamoto, K., Ishimoto, S., Minoda, R., Brough, D. E. & Raphael, Y. *J Neurosci* **23**, 4395-400 (2003).
53. Kanzaki, S., Ogawa, K., Camper, S. A. & Raphael, Y. *Hear Res* **169**, 112-20 (2002).
54. Ishimoto, S., Kawamoto, K., Kanzaki, S. & Raphael, Y. *Hear Res* **173**, 187-97 (2002).

55. Kawamoto, K., Oh, S. H., Kanzaki, S., Brown, N. & Raphael, Y. *Mol Ther* **4**, 575-85 (2001).
56. Springer, J. & Kitzman, P. in *Neuroprotective Signal Transduction* (ed. Mattson, M.) 1-21 (Humana Press Inc, Totowa, NJ, 1998).
57. Otte, J., Schunknecht, H. F. & Kerr, A. G. *Laryngoscope* **88**, 1231-46 (1978).
58. Webster, M. & Webster, D. B. *Brain Res* **212**, 17-30 (1981).
59. Altschuler, R. A., Cho, Y., Ylikoski, J., Pirvola, U., Magal, E. & Miller, J. M. *Ann N Y Acad Sci* **884**, 305-11 (1999).
60. Miller, J. M., Chi, D. H., O'Keeffe, L. J., Kruszka, P., Raphael, Y. & Altschuler, R. A. *Int J Dev Neurosci* **15**, 631-43 (1997).
61. Shinohara, T., Bredberg, G., Ulfendahl, M., Pyykko, I., Olivius, N. P., Kaksonen, R., Lindstrom, B., Altschuler, R. & Miller, J. M. *Proc Natl Acad Sci U S A* **99**, 1657-60 (2002).
62. Mitchell, A., Miller, J. M., Finger, P. A., Heller, J. W., Raphael, Y. & Altschuler, R. A. *Hear Res* **105**, 30-43 (1997).
63. Shepherd, R. K. & Hardie, N. A. *Audiol Neurootol* **6**, 305-18 (2001).
64. Araki, S., Kawano, A., Seldon, L., Shepherd, R. K., Funasaka, S. & Clark, G. M. *Laryngoscope* **108**, 687-95 (1998).
65. Li, L., Parkins, C. W. & Webster, D. B. *Hear Res* **133**, 27-39 (1999).
66. Lousteau, R. J. *Laryngoscope* **97**, 836-42 (1987).
67. Hartshorn, D. O., Miller, J. M. & Altschuler, R. A. *Otolaryngol Head Neck Surg* **104**, 311-9 (1991).
68. Leake, P. A., Hradek, G. T., Rebscher, S. J. & Snyder, R. L. *Hear Res* **54**, 251-71 (1991).
69. Hegarty, J. L., Kay, A. R. & Green, S. H. *J Neurosci* **17**, 1959-70 (1997).
70. Miller, A. L., Prieskorn, D. M., Altschuler, R. A. & Miller, J. M. *Brain Res* **966**, 218-30 (2003).
71. Yagi, M., Kanzaki, S., Kawamoto, K., Shin, B., Shah, P. P., Magal, E., Sheng, J. & Raphael, Y. *J Assoc Res Otolaryngol* **1**, 315-25 (2000).
72. Kanzaki, S., Stover, T., Kawamoto, K., Prieskorn, D. M., Altschuler, R. A., Miller, J. M. & Raphael, Y. *J Comp Neurol* **454**, 350-60 (2002).
73. Paasche, G., Gibson, P., Averbeck, T., Becker, H., Lenarz, T. & Stover, T. *Otol Neurotol* **24**, 222-7 (2003).
74. Tateya, I., Nakagawa, T., Iguchi, F., Kim, T. S., Endo, T., Yamada, S., Kageyama, R., Naito, Y. & Ito, J. *Neuroreport* **14**, 1677-81 (2003).
75. Hu, Z., Wei, D., Johansson, C. B., Holmstrom, N., Duan, M., Frisen, J. & Ulfendahl, M. *Exp Cell Res* **302**, 40-7 (2005).

BRAIN RESEARCH 1068 (2006) 237–247

available at www.sciencedirect.com

SCIENCE DIRECT®

www.elsevier.com/locate/brainres

BRAIN RESEARCH

Research Report

Nuclear factor-kappa B nuclear translocation in the cochlea of mice following acoustic overstimulation

Masatsugu Masuda[a,*], *Reiko Nagashima*[b], *Sho Kanzaki*[a], *Masato Fujioka*[a], *Kiyokazu Ogita*[b], *Kaoru Ogawa*[a]

[a]*Department of Otolaryngology, School of Medicine, Keio University, 35 Shinanomachi, Shinjuku-ku, Tokyo 160-8582, Japan*
[b]*Department of Pharmacology, Setsunan University, 45-1 Nagaotoge-cho, Hirakata, Osaka 573-0101, Japan*

ARTICLE INFO

Article history:
Accepted 2 November 2005
Available online 22 December 2005

Theme:
Sensory systems
Topic:
Auditory, vestibular, and lateral line: periphery

Keywords:
Cochlea
Inducible nitric oxide
Lateral wall
Noise trauma
Nuclear factor-kappa B
p65

ABSTRACT

There is increasing evidence to suggest that the expression of many molecules in the lateral wall of the cochlea plays an important role in noise-induced stress responses. In this study, activation of the nuclear transcription factor nuclear factor-kappa B (NF-κB) was investigated in the cochlea of mice treated with intense noise exposure (4 kHz, octave band, 124 dB, for 2 h). The present noise exposure led to remarkable auditory brainstem response threshold shifts and cochlear damage on surface preparations. To assess the effects of noise exposure on NF-κB/DNA binding activity in the cochlea, we prepared nuclear extracts from the cochlea at different time points after noise exposure and carried out an electrophoretic mobility shift assay using a probe specific to NF-κB. NF-κB/DNA binding was significantly enhanced in the cochlea 2–6 h after noise exposure and returned to basal levels after 12 h. Supershift analysis using antibodies against p65 and p50 proteins, which are components of NF-κB, demonstrated that enhancement of NF-κB/DNA binding was at least in part due to nuclear translocation of p65. An immunohistochemical study also showed that nuclear translocation of both p65 and p50 was observed in the lateral wall after noise exposure and that there may be a possible close association between p65 and enhanced inducible nitric oxide synthase expression. These results suggest that NF-κB may have a detrimental role in the response to acoustic overstimulation in the cochlea of mice.

* *Corresponding author.* Fax: +81 3 5379 0335.
E-mail address: masu13@sc.itc.keio.ac.jp (M. Masuda).

0006-8993/$ – see front matter © 2005 Elsevier B.V. All rights reserved.
doi:10.1016/j.brainres.2005.11.020

Abbreviations:
ABR, auditory brainstem response
AP-1, activator protein-1
Ca^{2+}, calcium
EAA, excitory amino acid
EMSA, electrophoretic mobility shift assay
IHC, inner hair cell
iNOS, inducible nitric oxide synthase
K^+, potassium
NF-κB, nuclear factor-kappa B
NO, nitric oxide
OC, organ of Corti
OHC, outer hair cell
PBS, phosphate-buffered saline
PFA, paraformaldehyde
PI, propidium iodide
ROS, reactive oxygen species
SPL, sound pressure level

1. Introduction

Intense noise exposure can lead to permanent damage to the sensory epithelium, the organ of Corti (OC), which includes sensory cells like the inner hair cells (IHCs) and outer hair cells (OHCs). The mechanisms of noise trauma are as follows: generation of nitric oxide (NO) or reactive oxygen species (ROS) leading to cytotoxicity to the sensory cells (Yamane et al., 1995; Ohlemiller et al., 1999; Ohinata et al., 2000; Nakashima et al., 2003; Shi and Nuttall, 2003); calcium (Ca^{2+}), potassium (K^+), and excitatory amino acid (EAA) overload leading to damage of sensory cells (Bohne and Rabbitt, 1983; Hsu et al., 2000; Jager et al., 2000; Hirose and Liberman, 2003; Hsu et al., 2004); and degeneration of the cochlear cells (Bohne and Rabbitt, 1983; Jager et al., 2000; Wang et al., 2002; Hirose and Liberman, 2003). There is a variety of evidence that the lateral wall, consisting of the spiral ligament and the stria vascularis, plays a critical role in these mechanisms.

Since a variety of stress responses occur, it is possible that simultaneous modulation of multiple mechanisms instead of a single mechanism can lead to better treatment outcomes for the hearing impairment resulting from noise trauma. This may be provided by modulation of transcription factors because one transcription factor regulates the expression of many genes in response to a single stimulus that induces tissue damage.

One of the most notable rapidly inducible transcription factors is nuclear factor-kappa B (NF-κB). NF-κB is composed of homo- and hetero-dimeric complexes of Rel family proteins including p65, p50, c-Rel, p52, and RelB. A hetero-dimer of p50/p65 is the predominant form of NF-κB (Bowie and O'Neill, 2000), however, a homodimer of p65/p65 or p50/p50 also exists (Ghosh et al., 1998). NF-κB exists in a latent form in the cytoplasm of unstimulated cells and is comprised of a transcriptionally active dimer bound to an inhibitor protein. Diverse stimulants lead to degradation of the NF-κB inhibitory protein and activation of NF-κB. The activated NF-κB dimer can then translocate into the nucleus and activate target genes by binding with high affinity to κB elements at their promoters. NF-κB plays a pivotal role in immune and inflammatory responses (Sha, 1998; Denk et al., 2000), neuronal development, neuronal cell death and survival, and neurodegeneration (Wooten, 1999; Denk et al., 2000; Mattson et al., 2000a,b).

Since activation of NF-κB induces both cytoprotective and cytotoxic proteins, the role of NF-κB in the mammalian cochlea has not been clearly determined. Jiang et al. reported that NF-κB protected murine cochlear hair cells from aminoglycoside-induced ototoxicity (Jiang et al., 2005). Ramkumar et al. suggested that NF-κB might protect the chinchilla cochlea from noise trauma because activation of NF-κB occurred in a similar time frame as the peak expression of the A1 adenosine receptor which acted in a protective role for the noise-exposed cochlea (Ramkumar et al., 2004). On the other hand, Merchant et al. suggested that human idiopathic sudden sensorineural hearing loss might be the result of abnormal activation of cellular stress pathways involving NF-κB (Merchant et al., 2005). Watanabe et al. suggested that apoptosis of cochlear cells was triggered by inducible nitric oxide synthase (iNOS)

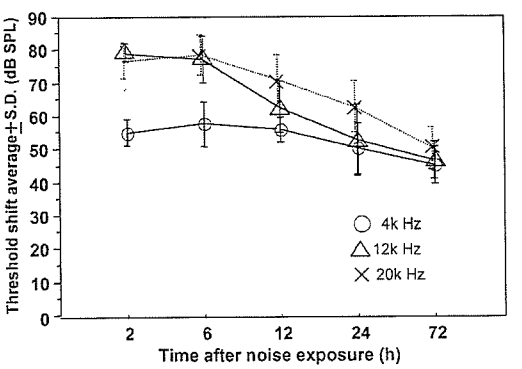

Fig. 1 – Changes in ABR thresholds after noise exposure with 124 dB SPL octave band noise, centered at 4 kHz, for 2 h of noise exposure. The graph shows remarkable ABR threshold elevations at the frequencies of 4, 12, and 20 kHz.

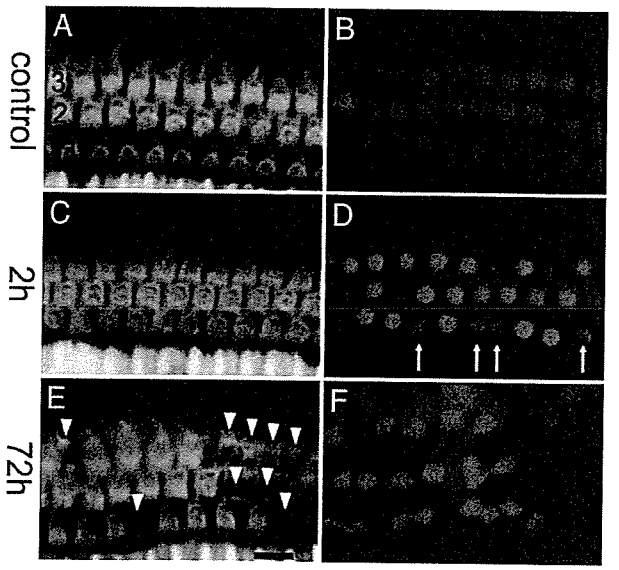

Fig. 2 – Surface preparations were obtained to confirm the cochlear damage. Flourescein phalloidin staining (A, C, E) was used to outline the OHCs. PI staining (B, D, F) was used to observe nuclear morphological change. (A, B) Preparations in the untreated mouse around the area of 50% of the distance from the apex to the base of the OC which is the area known to correspond to 10 kHz. These preparations show the regular outline of three rows of OHCs (A) and normal nuclear morphology (B). (C, D) Preparations in the mouse 2 h after noise exposure around the area of 50% of the distance of the OC. These preparations demonstrate the normal outlines of the OHCs (C), however, some nuclei have morphological changes (arrows in D) indicating damaged cells, even further away than 25%, which is the area known to correspond to 4 kHz, at only 2 h after noise exposure. (E, F) Preparations around the area of 25% of the OC of the mouse 72 h after noise exposure. They show loss of OHCs (E, arrow heads) and much more nuclear morphological changes than at 2 h after exposure. Scale bar = 10 μm.

through activation of NF-κB in cisplatin-treated mice (Watanabe et al., 2002). It was also reported that excess expression of iNOS followed by increased NO-related ROS contributes to noise-induced hearing loss (Shi and Nuttall, 2003; Shi et al., 2002, 2003; Ohinata et al., 2003). Therefore, there is also the possibility that NF-κB acts in a ototoxic role in noise trauma through the induction of enhanced iNOS expression. It has been shown that NF-κB was activated in the chinchilla cochlea after noise exposure (Ramkumar et al., 2004), however, the temporal and spatial aspects of activation were not evaluated. These aspects are important for transcription factors because their downstream targets may be stimulus-, temporal-, structure-, or cell type-specific. Activator protein-1 (AP-1), another notable transcription factor, is a very impressive example of this importance. Enhancement of AP-1/DNA binding activity 5 h after noise exposure is protective in the OC and the lateral wall, however, it is cytotoxic in the OC 15 h after exposure (Matsunobu et al., 2004). AP-1 activity is regulated by NF-κB (Fujioka et al., 2004), and activation of NF-κB and AP-1 leads to the coordinated expression of target genes (Rahman et al., 2004).

Therefore, we examined the time course of NF-κB activation with an electrophoretic mobility shift assay (EMSA), cellular localization, and immunohistochemistry to examine the possible association between NF-κB activation and induction of enhanced iNOS expression.

2. Results

2.1. *Auditory brainstem response threshold shift and surface preparation*

Cochlear damage was examined functionally by auditory brainstem responses (ABRs) and morphologically by surface preparations. The noise, 124 dB sound pressure level (SPL) octave band noise, centered at 4 kHz for 2 h, produced profound ABR threshold shifts at the frequencies of 4, 12, and 20 kHz from 2 h to 72 h after noise exposure (Fig. 1).

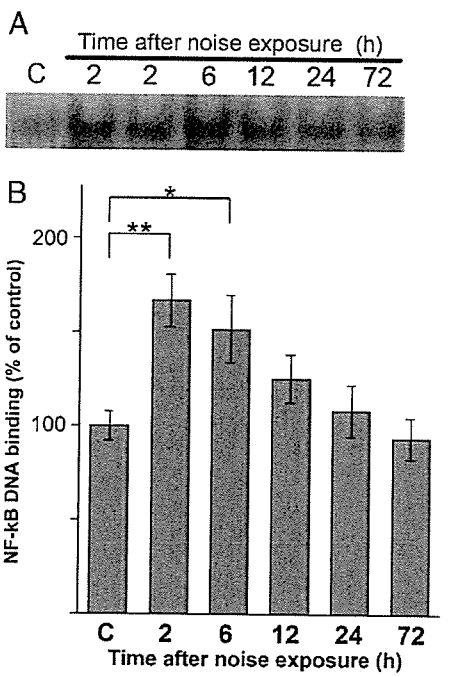

Fig. 3 – Time course of NF-κB/DNA binding activity after noise exposure. (A) NF-κB binding was analyzed by an EMSA as described in the text. The cochleae were processed after the resting times indicated on the figure (C, control). Bound probes are more intense in the cochleae 2–6 h after noise exposure than in the untreated cochleae and are less intense after 6 h. (B) Densitometric data. Autoradiograms were quantified by scanning with the NIH imaging software, and binding activities were normalized to the value prior to noise exposure. Values are expressed as the percent of the value prior to exposure; numbers are mean ± SE. **, * Significantly different from pre-exposure levels ($P < 0.01$ and *$P < 0.05$ by unpaired t test).**

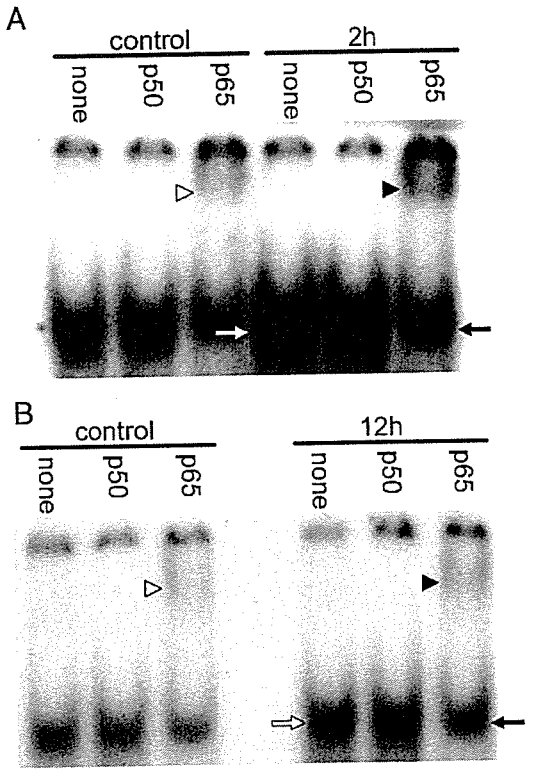

Fig. 4 – Supershift analysis of NF-κB/DNA binding. (A) Analysis of 2 h after noise exposure. (B) Analysis of 12 h after noise exposure. After incubation for NF-κB/DNA binding, the reaction mixture was further incubated for 16 h at 4 °C in the absence (none) or presence of 3 μg anti-p65 (p65) or anti-p50 (p50) antibody as described in the text. Migration of the probe/protein complex (black arrows and white arrows) is partially retarded (black arrow heads and white arrow heads) in the cochlea tissue after incubation with anti-p65 antibody. The supershifted band is more intense 2 h (A, black arrow head) after noise exposure than 12 h (B, black arrow head). The bands of the NF-κB/DNA probe not bound with antibody are also more intense in mice 2 h after noise exposure (white arrows) than those of untreated mice and of mice 12 h after noise exposure. This finding is consistent with the EMSA results.

The surface preparation from the untreated mouse showed a normal OHC outline (Fig. 2A) and a normal nucleus (Fig. 2B). Few OHC losses were observed in the cochlea 2 h after noise exposure (Fig. 2C), however, shrunken nuclear bodies, which indicated dying hair cells (Hu et al., 2002; Minami et al., 2004), were observed (Fig. 2D, arrows). The observed area was about 50% of the distance from the apex to the base where the OC was maximally vibrated by the 10 kHz tone (Ou et al., 2000). The morphological changes around the area of 50% of the distance were the same as the area of 25%, where the OC was maximally vibrated by the 4 kHz tone, 2 h after noise exposure. The cochlea was damaged even if the observed area was 50% of the distance from the apex, where the OC was not maximally vibrated by 4 kHz tone, 2 h after noise exposure. Seventy-two hours after the noise exposure, OHC losses were clearly observed around the area of 25% (Fig. 2E, arrow heads) and greater than 70% (data not shown) of the distance from the apex, and more shrunken nuclear bodies were observed than 2 h of noise exposure (Fig. 2F). The damage of the IHC was not found at any time point.

2.2. *Effects of noise exposure on NF-κB/DNA binding*

Nuclear extracts of the whole cochlea demonstrated binding of endogenous NF-κB to the radiolabeled oligonucleotide probe (Fig. 3A). Several control experiments confirmed the specificity of the observed binding. Gels showed no band in the absence of nuclear extracts or in the presence of excessive non-radioactive oligonucleotides probe. In contrast, the addition of an unlabeled double-stranded oligonucleotide probe lacking the consensus core element for NF-κB did not inhibit the binding of NF-κB (data not shown).

Binding activity was determined at various times up to 72 h after noise exposure in nuclear extracts of the cochlea (Figs. 3A, B). A clear elevation of the NF-κB/DNA binding activity was observed in the cochlea. Binding activity was significantly elevated about 1.7-fold 2 h after noise exposure and remained significantly elevated until 6 h after noise exposure and returned to near baseline levels 12 h after noise exposure.

2.3. *Protein composition of the NF-κB complex*

In order to evaluate the participation of NF-κB family proteins in NF-κB/DNA binding, nuclear extracts were individually incubated with antibodies against p65 and p50 prior to the incubation with the radiolabeled DNA probe. Because the highest increase in NF-κB/DNA binding was observed 2 h after noise exposure, this time point was selected for analysis. The time point of 12 h was also selected to confirm that the supershifted band would also return to near baseline levels and to confirm the result of the EMSA. Protein/antibody complexes bound to the DNA probe will shift the position of the complex on the gel to a higher molecular size, i.e. slower migration. Such a "supershift" was observed for p65 (Fig. 4, black arrow heads and white arrow heads), and the difference of the band intensity between untreated mice (Fig. 4, white arrow head) and noise-exposed mice (Fig. 4 black arrow head) was more clear after 2 h (Fig. 4A) than 12 h (Fig. 4B). The bands of NF-κB/DNA probe complexes of p65 were less intense (Fig. 4, black arrows) than those without antibodies (none in Fig. 4) and with an antibody for p50 (Fig. 4, white arrows) because a part of the complexes of p65 has translocated to the supershifted bands (Fig. 4, black arrow heads and white arrow heads).

When the hippocampal nuclear extracts were used as a sample in the supershift analysis, NF-κB/DNA binding was completely inhibited by the addition of anti-p50 antibody (data not shown). This meant that the anti-p50 antibody used in the present study was validated. In the case of the cochlea, however, binding of p50 was not significantly affected by preincubation with this antibody. These findings suggest that p65 is a major protein component of the NF-κB complex for DNA binding in untreated mice, whereas p50 is not. Following the 2 h of noise exposure, the p65 supershift was also evident, and the p50 supershift was not affected by the preincubation with the antibodies. Therefore, p65 may be a major component of the NF-κB binding activity following noise exposure.

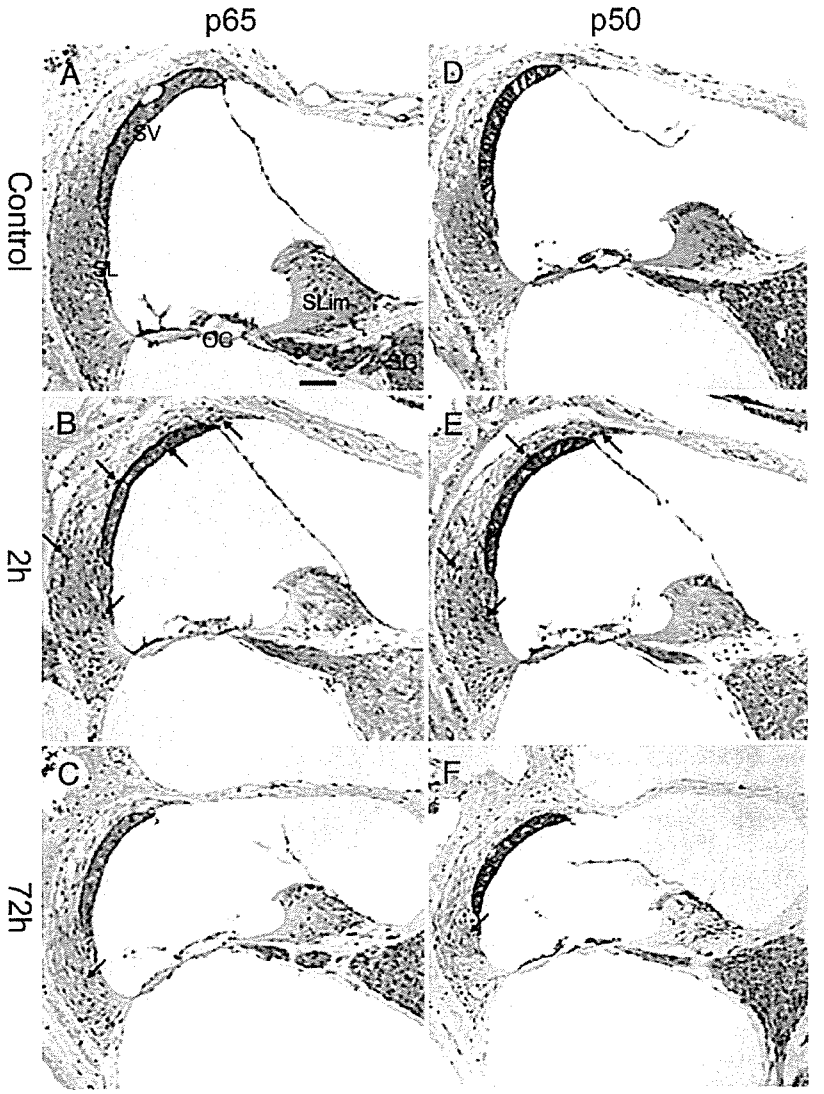

Fig. 5 – Comparison of immunolocalization of NF-κB in mid-modiolar sections in the cochlea of untreated mice (A, D) versus mice 2 h (B, E) and 72 h (C, F) after noise exposure. These sections were taken from the middle turn of the cochleae. There were no remarkable differences in the immunohistochemical staining pattern among the apical, middle, and basal turns. (A–C) Immunostaining for p65. (D–F) Immunostaining for p50. The cells of the lateral wall have darkly stained nuclei 2 h after noise exposure (arrows), indicative of NF-κB activation. On the other hand, the nuclei are not stained before noise exposure and become less intensely stained 72 h after noise exposure. The positive stain of the cytoplasm indicates the latent form of NF-κB. Scale bar = 50 μm. Scale bar applies to A–F.

The difference of the band intensity of NF-κB/DNA probe complex between untreated mice and noise-exposed mice was more clear after 2 h (Fig. 4A, white arrows) than after 12 h (Fig. 4B, white arrows). This was consistent with the EMSA results.

2.4. *p65 and p50 immunostaining in the cochlea*

Figs. 5 and 6 show immunolocalization of p65 (Figs. 5A–C, 6) and p50 (Figs. 5D–F) in mouse cochlea 2 h (Figs. 5B, E, 6) and 72 h (Figs. 5C, F) after noise exposure and in the unexposed cochlea (Figs. 5A, D). There was little or no nuclear immunostaining for p65 and p50 in the unexposed cochlea. On the other hand, prominent nuclear localization of these antibodies occurred in the lateral wall 2 h after noise exposure (Figs. 5B, E), and then the nuclear immunostaining became much less intense 72 h after (Figs. 5C, F). Immunostaining translocations from the cytoplasms in untreated mice into the nuclei of noise-exposed mice for p65 were seen in cells of the spiral ligament and of the stria vascularis. As for p50, the translocation was seen in the spiral ligament but was not clearly seen in the stria vascularis. Cytoplasm immunostaining with these antibodies was found in the cells of the OC (Fig. 6), the spiral limbus, and the spiral ganglion (Fig. 5) in both the noise-exposed and the untreated cochlea, although the clear immunostaining shift from the cytoplasm into the nucleus did not occur in noise-exposed cochlea. Along the cochlear spiral, the

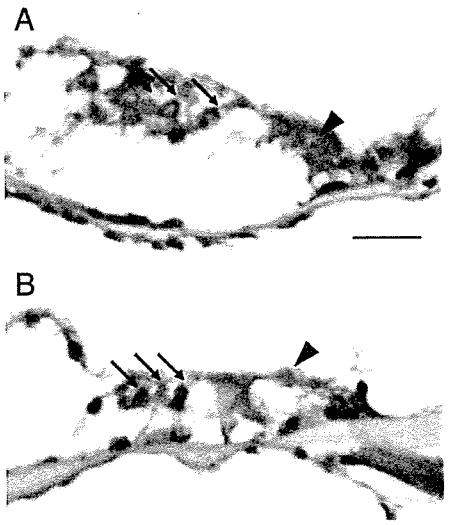

Fig. 6 – Comparison of immunolocalization of p65 in the OC between the apical turn (A) and the middle turn (B) 2 h after noise exposure. Along the cochlear spiral and the lateral wall, the immunostaining pattern of the OC was homogeneous. There was no difference in the immunohistochemical staining pattern of p65 and p50 in the OC at any time point. Arrow, OHC; arrow head, IHC. Scale bar = 20 μm. The scale bar applies to A and B.

immunostaining pattern of the lateral wall was homogeneous from the apex to the base. This homogenous pattern was also seen in the other parts, including the OC (Fig. 6). Both the OC of the apical turn (Fig. 6A) and the middle turn (Fig. 6B) lacked nuclear immunostaining for p65 after noise exposure. There was no difference in the immunohistochemical staining pattern of the OC with either p65 or p50. When the primary antibody was omitted, no staining was observed in the noise-exposed cochlea (data not shown).

The remarkable morphological differences in the lateral wall tissue of the slides from the different time points were not seen.

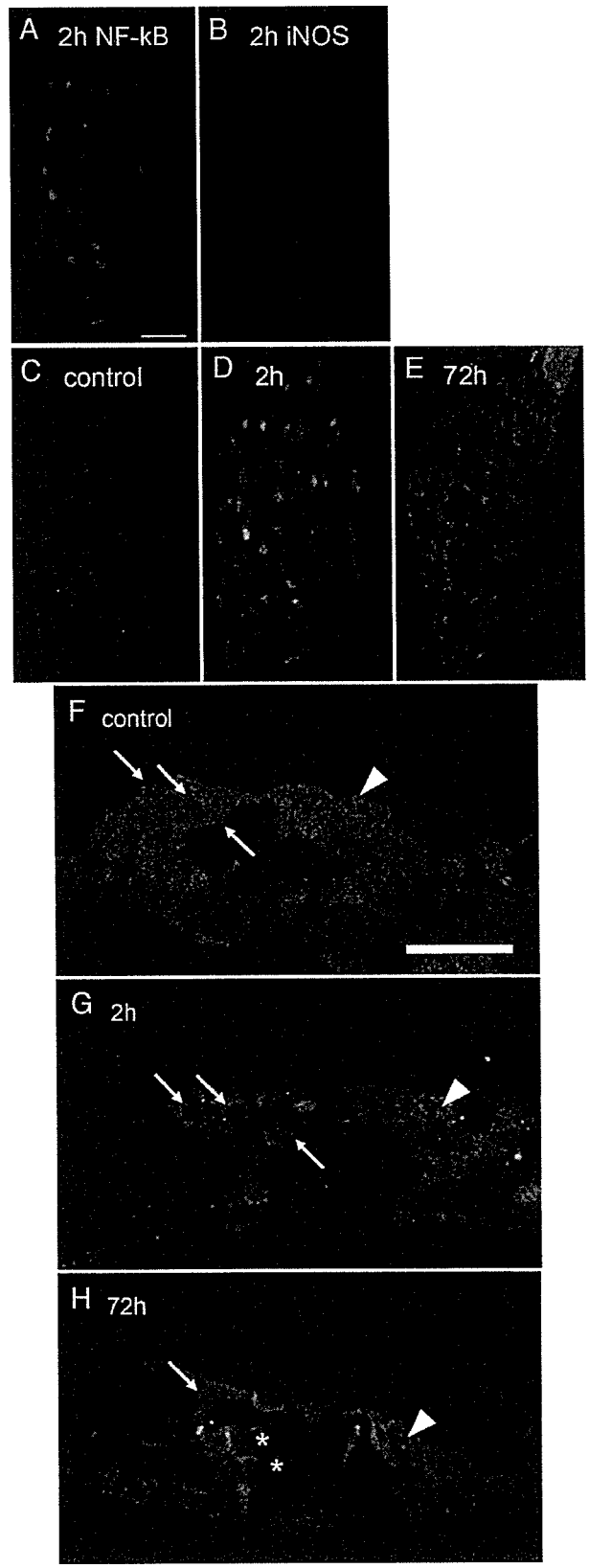

Fig. 7 – Double labeling immunohistochemistry was used to observe the relationship between NF-κB activation (A) and iNOS production (B) in the NF-κB activated cells of the lateral wall (A–E) and the cells of the OC (F–H). (C–H) Merged images of NF-κB (green) and iNOS (red). The sections were taken from the middle turn. There was no remarkable difference in the immunohistochemical staining pattern among the apical, middle, and basal turns. Most of the cells that had positive nuclear staining for p65, which is indicative of NF-κB activation, also stained positive for iNOS (D, yellow) in the mice 2 h after noise exposure. Double labeled cells (yellow) were not seen in the untreated mice (C), and weak double immunoreactivity in the cytoplasm was seen in the mice 72 h after noise exposure (E). In the OC, p65 immunolocalized (green or yellow) to the cytoplasm, and there was no clear immunolocalization shift into the nuclei of sensory cells, which consisted of IHCs (arrows) and OHCs (arrow heads) and other cells of the OC at 2 h (G) and at 72 h (H) after noise exposure. Damaged OHCs are observed (*). Scale bar = 25 μm. The scale bar in figure A applies to A–E. The scale bar in figure F applies to F–H.

2.5. *iNOS immunoreactivity in the p65 activated cells*

The supershift analysis revealed that a major component of the NF-κB binding activity following noise exposure was p65, and the immunohistochemical study revealed that the activation was prominent in the spiral ligament of the lateral wall. Therefore, a double labeling immunohistochemical study for p65 and iNOS in the spiral ligament was conducted to explore the possibility that NF-κB regulated iNOS expression in the noise-exposed cochlea.

In the lateral wall of mice 2 h after noise exposure, most of the NF-κB activated cells, which demonstrated nuclear immunostaining for p65 (Fig. 7A, green), also showed positive immunostaining for iNOS (Fig. 7B, red). Furthermore, the colocalization of p65 and iNOS was observed as strong yellow nuclear immunostaining in the merged image (Fig. 7D). In the lateral wall of untreated mice, no significant colocalization was observed (Fig. 7C). In the lateral wall of mice 72 h after noise exposure, weak colocalization was observed in the cytoplasm (Fig. 7E).

In the OC, no nuclear staining for p65 or iNOS was observed at any time point (Figs. 7F–H). These sections were from the middle turn of the cochleae. There were no remarkable differences in the immunohistochemical staining pattern in the apical, middle, and basal turns. When the primary antibody was omitted, no staining was observed in the noise-exposed cochlea (data not shown).

3. Discussion

The present study provides evidence that NF-κB/DNA binding in the mammalian cochlea is increased, with a peak level around 2 h after the end of the noise exposure, and indicates that there is a possible close association between NF-κB activation and iNOS expression following noise overstimulation.

The present noise condition resulted in noise-induced cochlear damage. It was confirmed by functional (Fig. 1) and histological (Fig. 2) studies with ABR and surface preparations respectively. The damage of the cochlea occurred throughout the area of greater than 25% of the distance from the apex to the base. The present distribution of OHC losses and/or nuclear condensation at 2 h after noise exposure was consistent with previous studies on noise-induced cellular injury in the mammalian cochlea (Hu et al., 2002; Wang et al., 2002; Minami et al., 2004). Since the present condition damaged the wide range of cochlear spiral, the immunostaining pattern was homogenous throughout the cochlea. Under this noise condition, the results of the immunohistochemical staining suggested a marked elevation of NF-κB/DNA binding in the lateral wall tissues, while no significant changes were observed in the OC and the spiral ganglion.

NF-κB is activated by oxidative stress, thereby acting as a "stress sensor" (Mattson et al., 2000a). The lateral wall is critical for normal functioning of the cochlea and for many pathologies including noise trauma, although the lateral wall is not a sensory epithelium like the OC. Examples of the crucial roles of the lateral wall are activation of a transcription factor such as AP-1 (Ogita et al., 2000; Shizuki et al., 2002; Matsunobu et al., 2004); generation of NO and ROS (Yamane et al., 1995; Ohinata et al., 2000; Takumida and Anniko, 2001; Nakashima et al., 2003; Ohinata et al., 2003; Shi and Nuttall, 2003); production of antioxidant enzymes (Jacono et al., 1998; Yamasoba et al., 1998; Ohlemiller et al., 1999); clearance of EAA (Li et al., 1994); and maintenance of electrochemical homeostasis (Spicer and Schulte, 1996; Hsu et al., 2000; Ichimiya et al., 2000; Kikuchi et al., 2000; Suko et al., 2000; Hsu et al., 2004). The lateral wall tissues may increase metabolic activity to maintain the above functions. There is compelling evidence that the lateral wall normally does not sustain permanent damage, however, their transiently increased metabolic activity might result in formation of free radicals after noise exposure (Yamane et al., 1995). Since NF-κB is a redox-sensitive transcription factor like AP-1 and acts as a "stress sensor" (Mattson et al., 2000a), the oxidative stress in the lateral wall may lead to NF-κB activation. The lateral wall responses mentioned above and NF-κB activation showed in the present study are also temporally consistent because the responses in the lateral wall after noise overstimulation mentioned above were initiated during noise exposure or within a few hours after the end of noise exposure. The peak level of NF-κB activation also occurred in the same time frame as shown in the present study.

In addition to these close associations among NF-κB, noise trauma, and the lateral wall, the present study showed that NF-κB activated cells had increased iNOS expression (Fig. 7). Increased iNOS expression leads to excess NO production. Excess NO leads to the formation of peroxynitrite, a powerful oxidant. Finally, cell death may be initiated by many mechanisms, including lipid peroxidation, protein nitration, DNA damage, or the irreversible inhibition of respiration (Keynes and Garthwaite, 2004). It was suggested that the iNOS-dependent cell injury mechanisms were associated with noise-induced hearing loss (Ohinata et al., 2003; Shi and Nuttall, 2003; Shi et al., 2003). Since NO induced by iNOS readily permeates tissue and can diffuse hundreds of microns away from the source where it was generated (Pryor et al., 1997), the present NF-κB stimulating iNOS expression in the lateral wall can result in oxidative stress in the whole cochlea. This suggests a possible detrimental role of NF-κB in the whole cochlea after noise overstimulation. For example, there is evidence that glucocorticoids inhibit NF-κB mediated molecular expression and provide therapeutic effects for central nervous system disease, sepsis, myocardial disease, hepatitis, and rheumatic disease (Handel, 1997; Xu et al., 1998; D'Acquisto et al., 2002; Garside et al., 2004). As for the cochlea, glucocorticoid administration during or immediately after noise overstimulation has protective effects in the mammalian cochlea (Mori et al., 2004; Takemura et al., 2004; Wang and Liberman, 2002). These glucocorticoid effects indicate that NF-κB activation can damage the noise-exposed cochlea.

However, the lateral wall cells showed no remarkable morphological change with NF-κB activation though they had robust iNOS expression (Figs. 7C–E). On the other hand, the OC was damaged without NF-κB activation (Figs. 7F–H). Considering that NF-κB activated cells were not damaged, NF-κB might play a protective role in each cell level. This consideration is consistent with the protective role of NF-κB in aminoglycoside-induced ototoxicity (Jiang et al., 2005). OHC death of the murine

cochlea induced by aminoglycoside antibiotics is mediated by ROS and can be prevented by antioxidants. Jiang et al. showed that NF-κB was not activated in OHCs of aminoglycoside-treated mice without antioxidants, however, it was activated there by cotreatment with antioxidants.

We cannot fully explain why the IHC had no morphological change and no nuclear immunostaining for NF-κB. There must be NF-κB-independent cytoprotective and/or cytotoxic pathways after noise exposure, and the balance between NF-κB-dependent and -independent pathways must determine the degree of the noise trauma.

As mentioned above, the role of the transcription factor is structure or cell type-specific, therefore, evaluation of its spatial aspects, as in the present study, is very important. AP-1 was quantified in the OC, lateral wall, and spiral ganglion independently along the time course. There is evidence that AP-1 has differential roles in the OC and the lateral wall and even in the OC at different times (Ogita et al., 2000; Shizuki et al., 2002; Matsunobu et al., 2004). Therefore, future studies of NF-κB-related pathways must quantify several components of the NF-κB family.

Some of the staining pattern for iNOS was not consistent with previous reports. Our data showed iNOS expression in the spiral ligament. Watanabe et al. also showed NF-κB activation and iNOS expression in the lateral wall in cisplatin-treated mice (Watanabe et al., 2002), however, Shi et al. showed iNOS expression in the stria vascularis but not in the spiral ligament in the lateral wall after noise exposure (Shi et al., 2003). This dissimilar result could be due to different techniques employed and the noise condition. For example, we fixed the cochlea by local perfusion only; on the other hand, the others fixed with cardiac perfusion. Second, we and Watanabe et al. fixed the cochlea with 4% PFA overnight and used paraffin embedding; on the other hand, Shi et al. used surface preparation fixed with 4% PFA for 4 h. Third, the noise conditions were different. The noise used in the study by Shi et al. was 110 dB SPL broad band noise, 3 h/day, for three consecutive days. This was far different from our noise condition described in Experimental procedures.

The results of the supershift and immunohistochemistry analyses indicate that the increase in NF-κB/DNA binding in the lateral wall is, at least in part, due to enhanced activation of p65. Although densitometric data show no significant differences in NF-κB/DNA activity between 72 h after noise exposure and lack of exposure (Fig. 3B), immunohistochemical staining suggest that p65 may still work at this time point (Fig. 5C) to some degree.

The supershift analysis of p50 indicates that p50 is not a component of NF-κB in the noise-exposed mouse cochlea. However, there were intense nuclear immunoreactivities of p50 2 h after noise exposure and less intense nuclear immunoreactivities 72 h after noise exposure (Figs. 5E, F). There may be several reasons for the inconsistency between the EMSA data and the immunohistochemical studies for p50. It is possible that different homodimers like p65/p65 or p50/p50 are implicated in noise trauma. The p65/p65 homodimer can translocate into the nucleus and bind the κB element in the noise-exposed cochlea. On the other hand, p50/p50 can translocate into the nucleus, however, it cannot bind the κB element in the noise-exposed cochlea. Therefore, immunolocalization of p50 was shown in the nucleus; however, the supershifted band was not seen in the supershift assay. Nuclear immunostaining translocation from the cytoplasm into the nucleus for p65 was clearly seen in the stria vascularis; however, it was not seen for p50. This difference in immunoreactivity between p65 and p50 in the stria vascularis may come from the existence of different NF-κB dimers as mentioned above in the cochlea.

In summary, NF-κB has the potential to play a detrimental role in the noise-exposed cochlea through the expression of iNOS, and the activation of NF-κB in response to noise exposure selectively occurs in the lateral wall in the early time frame. On the other hand, it has the potential to play a protective role in each cell of the lateral wall. Therefore, further evaluations will be needed before NF-κB becomes a target of the treatment of noise-induced hearing loss.

4. Experimental procedures

4.1. *Experimental groups and experimental design*

Mice used in this study were male C57BL/6 J mice obtained from the Saitama-experimental animal center (Saitama, Japan) and entered into the study at 5 weeks of age. Cochlear function was tested in each animal via measurement of ABRs. Animals were randomly assigned to either a matrix of noise exposure or a control group receiving no noise exposure. First, we conducted an EMSA to investigate the activation of NF-κB/DNA binding in the mouse cochlea after noise exposure. Second, we conducted supershift analysis to analyze the composition of NF-κB proteins bound to the DNA probe. Third, we conducted immunohistochemistry to study the cellular localization of NF-κB and the relationship between NF-κB and iNOS in the mouse cochlea after noise exposure and in the cochlea unexposed to noise. For the EMSA, the numbers of analyzed ears were $n = 8$ for control, $n = 8$ for 2 h, $n = 8$ for 6 h, $n = 8$ for 12 h, $n = 8$ for 24 h, and $n = 9$ for 72 h after noise exposure. A mixture of nuclear extracts remaining after the EMSA analysis at each time point was used for supershift analysis of control, 2 h, and 12 h after noise exposure. For immunohistochemistry, the numbers of analyzed ears were $n = 2$ for control, $n = 2$ for 2 h, and $n = 2$ for 72 h after noise exposure.

4.2. *Noise exposure*

Mice were exposed to 124 dB SPL octave band noise, centered at 4 kHz, for 2 h, within a sound chamber. Each animal was placed in a cage. The sound chamber was fitted with a speaker driven by a noise generator (AA-67N; RION, Tokyo, Japan) and two power amplifiers (SRP-P150; SONY, Tokyo, Japan and D-1405; FOSTEX, San Angelo Drive Chesterfield, MO, USA). To ensure uniformity of the stimulus, sound levels were calibrated and measured using a sound level meter (NL-20; RION, Tokyo, Japan). The sound level meter was positioned at the level of the animal's head.

4.3. *Auditory brainstem response recording*

For ABR measurement, stainless steel needle electrodes were placed at the vertex and ventro-lateral to the left and right ears. Electroencephalogram recording was performed using the extracellular amplifier Digital Bioamp system (BAL-1; Tucker-Davis Technologies, FL, USA), and waveform storing and stimulus control were performed using Scope software of PowerLab system (PowerLab 2/20; ADInstruments, Castle Hill, Australia). Sound stimuli were produced by a coupler type speaker (ES1spc;

BioResearchCenter, Nagoya, Japan) inserted into the external auditory canal of a mouse. Tone burst stimuli, 0.1 ms rise/fall time (cosine gate) and 1 ms flat segment, were generated using Real-Time Processor (RP2.1; Tucker-Davis Technologies, FL, USA), and the amplitudes were specified by a Programmable Attenuator (PA5; Tucker-Davis Technologies, FL, USA). Sound levels were calibrated using a sound level meter (LA-5111; Ono Sokki, Yokohama, Japan). ABR waveforms were recorded for 12.8 ms at a sampling rate of 40,000 Hz using 50–5000 Hz bandpass filter settings. Waveforms from 1024 stimuli at a frequency of 9 Hz were averaged. For recording, animals were anesthetized (80 mg/kg ketamine, 15 mg/kg xylazine, i.p.). The thresholds of ABR were determined before noise exposure and 2 h, 6 h, 12 h, 24 h, or 72 h afterward at 4, 12, and 20 kHz, using a 5-dB SPL minimum step size down from a maximum amplitude. The hearing threshold was defined as the lowest stimulus intensity that produced a reliable wave III of ABR. Because the constraining test tones were set to SPLs of less than 89.7, 86.7, and 85 dB at 4, 12, and 20 kHz, respectively, the thresholds were recorded as 94.7, 91.7, and 90 dB respectively for the calculation of the threshold shift value when there was no response due to profound hearing impairment.

4.4. *Surface preparation*

Surface preparations were carried out to ensure whether this noise condition damaged the cochlea. The numbers of analyzed ears were $n = 1$ for control, $n = 2$ for 2 h, and $n = 2$ for 72 h after noise exposure. These animals were not used for other procedures. The auditory bullae were quickly removed, and the inner ear was transferred into 4% paraformaldehyde (PFA). The bones near the apex of the cochlea as well as the round window and oval window were opened followed by perilymphatic perfusion with 4% PFA. After overnight fixation at 4 °C, the inner ears were decalcified in 0.1 M EDTA for 7 days. After removal of the bony capsule and the lateral wall tissues, the OC was removed from the temporal bone. Tissue was incubated in 0.3% Triton X-100 in PBS for 7 min. The OC was incubated with flourescein phalloidin (F-432; Molecular Probes, Eugene, OR, USA; 1:50) overnight to outline hair cells. After three PBS rinses, the OC was incubated with propidium iodide (PI) (P-3566; Molecular Probes; 1:250) for 15 min to evaluate nuclear morphology. After three PBS rinses, it was mounted as a surface preparation. The areas around 25% and 50% of the distance from the apex, which are known to be the most stimulated regions by the 4 kHz and 10 kHz sounds, respectively (Ou et al., 2000), were observed. The area that was 70% of the distance from the apex, which is known to be vulnerable to noise exposure regardless of the center frequency of the octave band noise (Ou et al., 2000; Wang et al., 2002), was also observed. Immunolabeling was visualized using epi-fluorescence microscopy.

4.5. *Sample preparation for EMSA*

Mice were immediately decapitated under deep anesthesia after ABR measurements, and then the cochleas were dissected to prepare nuclear extracts according to Schreiber et al. (1989) with minor modifications (Ogita et al., 2000). In brief, tissues were homogenized in 10 mM sodium HEPES (pH 7.9) containing 10 mM KCl, 1 mM EDTA, 1 mM EGTA, 5 mM dithiothreitol, the phosphatase inhibitors (10 mM sodium β-glycerophosphate and 1 mM sodium orthovanadate), and 1 μg/ml each of the protease inhibitors (*p*-amidinophenyl) methanesulfonyl fluoride, benzamidine, leupeptin, and antipain. After the addition of Nonidet P-40 at a final concentration of 0.5%, the homogenates were centrifuged at 15,000 × *g* for 5 min to pellet a nuclei-containing fraction. The pellets were suspended in 50 mM Tris–HCl (pH 7.5) containing 10% glycerol, 400 mM NaCl, 1 mM EDTA, 1 mM EGTA, 5 mM dithiothreitol, and the phosphatase and protease inhibitors as above and kept on ice for 30 min. The suspensions were then centrifuged at 15,000 × *g* for 5 min, and the supernatant nuclear extracts were stored at −80 °C until assay.

4.6. *NF-κB/DNA binding mobility shift assays*

Oligonucleotides containing the NF-κB binding sequence from the murine κ-immunoglobulin light chain gene enhancer, 5′-AGTTGAGGGGACTTTCCCAGG-3′, and its complementary sequence were annealed as a probe for the EMSA. The probe was labeled with [α-^{32}P]deoxy-ATP (PerkinElmer Life Sciences, Inc., MA, USA) using Klenow fragment of DNA polymerase I in 10 mM Tris–HCl buffer (pH 7.5) containing 50 mM NaCl, 10 mM $MgCl_2$, and 1 mM DTT at 25 °C for 30 min in the presence of 50 μM each of deoxy-GTP, deoxy-CTP, and deoxy-TTP. Aliquots (5 μg of protein) of nuclear extracts were incubated with 50 fmol probe ($0.5–5 \times 10^6$ cpm/pmol) in 20 μL 50 mM Tris–HCl buffer (pH 7.5) containing 1 μg poly(dI–dC), 10% (vol/vol) glycerol, 10 mM $MgCl_2$, 160 mM NaCl, 1 mM EDTA, 1 mM EGTA, 5 mM DTT, 5 mM each of the aforementioned phosphatase inhibitors, and 1 μg/mL each of the protease inhibitors for 30 min at 2 °C. Bound and free probes were separated by electrophoresis on a 5% (wt/vol) polyacrylamide gel in buffer (pH 8.5) containing 50 mM Tris, 0.38 M glycine, and 2 mM EDTA at a constant voltage of 11 V/cm for 1.5 h in an ice bath. Gels were fixed, dried, and exposed to X-ray films for different periods to obtain autoradiograms most adequate for subsequent quantitative densitometry.

4.7. *Determination of NF-κB protein component by supershift analysis*

The composition of proteins bound to the DNA probe was analyzed by preincubation of nuclear extracts with antibodies against individual components of the NF-κB protein family including p50 and p65 proteins. Antibodies against p50 (sc-7178; Santa Cruz Biotechnology Inc., Santa Cruz, CA, USA; 3 μg) or p65 (sc-109-G; Santa Cruz Biotechnology Inc.; 3 μg) were added into the incubation mixture and allowed to react at 4 °C for 14–16 h. Samples were then subjected to electrophoresis (as described above), and autoradiograms were analyzed for supershift of the bound probe to a more slowly migrating position due to antibody association with the complex (Ogita et al., 1996).

4.8. *Data analysis and statistics*

Densitometric analysis for quantification of autoradiograms was carried out with the aid of Atto Densitograph (Atto Co., Tokyo, Japan). Values for each tissue were calculated as the percentage of NF-κB/DNA binding in noise-exposed mice compared with untreated mice and are expressed as the mean ± SE. Statistical significance was determined by Student's *t* test using Stat-View software (SAS Institute, Inc., Cary, NC, USA), and differences with *P* value less than 0.05 were considered significant.

4.9. *Immunohistochemistry for NF-κB*

For immunohistochemistry, mice were immediately decapitated under deep anesthesia after ABR measurements. The auditory bullae were quickly removed and the inner ear transferred into 4% PFA. Perilymphatic perfusion with 4% PFA was performed as described above. After overnight fixation at 4 °C, the inner ears were decalcified in 0.1 M EDTA for 7 days and embedded in paraffin using routine procedures and sectioned at 4 μm thickness. The slides were dewaxed in xylene, rehydrated through graded ethanol, and quenched with 3% H_2O_2 in methanol for 30 min. After antigen retrieval by heat treatment in 10 mM citrate buffer (pH 6.0) at 105 °C for 45 min, they were quenched with 0.1% avidin for 20 min, 0.01% biotin for 20 min, and 1% casein for 30 min.

Immunolabeling was carried out overnight at 4 °C with an anti-p65 antibody (sc-372; Santa Cruz Biotechnology Inc.; 1:50) or an anti-p50 antibody (KAP-TF112; Stress Gen Biotechnologies Corp., Glanford Avenue Victoria, BC, Canada; 1:200), and then the slides were incubated for 30 min in biotinylated anti-goat IgG antibody (AP106B; Chemicon International, Temecula, CA, USA; 1:200) for p65 and in biotinylated anti-rabbit IgG antibody (BA-1000; Vector Laboratories, Burlingame, CA, USA; 1:200) for p50 at room temperature. Finally, the slides were incubated for 30 min in Streptavidin ABComplex/HRP (K0377; Dako, Glostrup, Denmark; 1:100). Reaction products were developed using 3′,5′-diaminobenzidine as a substrate for peroxidase. Sections were nuclear stained with hematoxylin. All of the washes were performed in 0.1 mM Tris-buffered saline (0.3M NaCl, 0.1% Tween20, 0.1 M Tris–HCl buffer) (pH 7.6) except for the wash after incubation in Streptavidin ABComplex/HRP. Tris-buffered saline of 50 mM (pH 7.6) was used for this wash.

4.10. *Immunohistochemistry for p65 and iNOS*

The paraffin slides, which were made in the above procedure, were dewaxed. After antigen retrieval by heat treatment in 10 mM citrate buffer (pH 6.0) at 105 °C for 30 min, they were incubated in blocking solution consisting of 1% casein for 30 min.

Immunolabeling was carried out for 1 h in room temperature with an anti-p65 antibody, and then the slides were incubated for 1 h in Alexa Fluor 488-conjugated rabbit anti-goat IgG secondary antibody (A-11078; Molecular Probes; 1:200). Next, immunolabeling for iNOS was carried for 1 h with an anti-iNOS antibody (SA-200; BIOMOL International, Plymouth Meeting, PA, USA; 1:500), and then the slides were incubated for 1 h in Alexa Fluor 546-conjugated F(ab′) fragment of goat anti-rabbit IgG secondary antibody (A-11071; Molecular Probes; 1:200). Sections were nuclear stained with hematoxylin. All of the washes were performed in 0.1 mM Tris-buffered saline (pH 7.6). Immunolabeling was visualized using confocal microscopy.

4.11. *Animal use and care*

All experimental protocols were in compliance with guidelines of the National Institutes of Health and the Declaration of Helsinki, and all procedures were approved and supervised by the Keio University Union on Laboratory Animal Medicine.

Acknowledgment

The author would like to thank Mr. Takashi Kimura for his assistance in immunohistochemistry.

REFERENCES

Bohne, B.A., Rabbitt, K.D., 1983. Hear. Res. 11, 41–53.
Bowie, A., O'Neill, L.A., 2000. Biochem. Pharmacol. 59, 13–23.
D'Acquisto, F., May, M.J., Ghosh, S., 2002. Mol. Interv. 2, 22–35.
Denk, A., Wirth, T., Baumann, B., 2000. Cytokine Growth Factor Rev. 11, 303–320.
Fujioka, S., Niu, J., Schmidt, C., Sclabas, G.M., Peng, B., Uwagawa, T., Li, Z., Evans, D.B., Abbruzzese, J.L., Chiao, P.J., 2004. Mol. Cell. Biol. 24, 7806–7819.
Garside, H., Stevens, A., Farrow, S., Normand, C., Houle, B., Berry, A., Maschera, B., Ray, D., 2004. J. Biol. Chem. 279, 50050–50059.
Ghosh, S., May, M.J., Kopp, E.B., 1998. Annu. Rev. Immunol. 16, 225–260.
Handel, M.L., 1997. Inflamm. Res. 46, 282–286.
Hirose, K., Liberman, M., 2003. J. Assoc. Res. Otolaryngol. 4, 339–352.
Hsu, C.J., Shau, W.Y., Chen, Y.S., Liu, T.C., Lin-Shiau, S.Y., 2000. Hear. Res. 142, 203–211.
Hsu, W.C., Wang, J.D., Hsu, C.J., Lee, S.Y., Yeh, T.H., 2004. Acta Oto-Laryngol. 124, 459–463.
Hu, B.H., Henderson, D., Nicotera, T.M., 2002. Hear. Res. 166, 62–71.
Ichimiya, I., Yoshida, K., Hirano, T., Suzuki, M., Mogi, G., 2000. Int. J. Pediatr. Otorhinolaryngol. 56, 45–51.
Jacono, A.A., Hu, B., Kopke, R.D., Henderson, D., Van De Water, T.R., Steinman, H.M., 1998. Hear. Res. 117, 31–38.
Jager, W., Goiny, M., Herrera-Marschitz, M., Brundin, L., Fransson, A., Canlon, B., 2000. Exp. Brain Res. 134, 426–434.
Jiang, H., Sha, S.H., Schacht, J., 2005. J. Neurosci. Res. 79, 644–651.
Keynes, R.G., Garthwaite, J., 2004. Curr. Mol. Med. 4, 179–191.
Kikuchi, T., Kimura, R.S., Paul, D.L., Takasaka, T., Adams, J.C., 2000. Brain Res. Brain Res. Rev. 32, 163–166.
Li, H.S., Niedzielski, A.S., Beisel, K.W., Hiel, H., Wenthold, R.J., Morley, B.J., 1994. Hear. Res. 78, 235–242.
Matsunobu, T., Ogita, K., Schacht, J., 2004. Neuroscience 123, 1037–1043.
Mattson, M.P., Culmsee, C., Yu, Z., Camandola, S., 2000a. J. Neurochem. 74, 443–456.
Mattson, M.P., Culmsee, C., Yu, Z.F., 2000b. Cell Tissue Res. 301, 173–187.
Merchant, S.N., Adams, J.C., Nadol Jr., J.B., 2005. Otol. Neurotol. 26, 151–160.
Minami, S.B., Yamashita, D., Schacht, J., Miller, J.M., 2004. J. Neurosci. Res. 78, 383–392.
Mori, T., Fujimura, K., Yoshida, M., Suzuki, H., 2004. Auris, Nasus, Larynx 31, 395–399.
Nakashima, T., Naganawa, S., Sone, M., Tominaga, M., Hayashi, H., Yamamoto, H., Liu, X., Nuttall, A.L., 2003. Brain Res. Brain Res. Rev. 43, 17–28.
Ogita, K., Amizuka, T., Azuma, Y., Yoneda, Y., 1996. Neurochem. Res. 21, 201–209.
Ogita, K., Matsunobu, T., Schacht, J., 2000. NeuroReport 11, 859–862.
Ohinata, Y., Miller, J.M., Altschuler, R.A., Schacht, J., 2000. Brain Res. 878, 163–173.
Ohinata, Y., Miller, J.M., Schacht, J., 2003. Brain Res. 966, 265–273.
Ohlemiller, K.K., Wright, J.S., Dugan, L.L., 1999. Audiol. Neuro-Otol. 4, 229–236.
Ou, H.C., Harding, G.W., Bohne, B.A., 2000. Hear. Res. 145, 123–129.
Pryor, W.A., Lemercier, J.N., Zhang, H., Uppu, R.M., Squadrito, G.L., 1997. Free Radical Biol. Med. 23, 331–338.
Rahman, I., Marwick, J., Kirkham, P., 2004. Biochem. Pharmacol. 68, 1255–1267.
Ramkumar, V., Whitworth, C.A., Pingle, S.C., Hughes, L.F., Rybak, L. P., 2004. Hear. Res. 188, 47–56.
Schreiber, E., Matthias, P., Muller, M.M., Schaffner, W., 1989. Nucleic Acids Res. 17, 6419.
Sha, W.C., 1998. J. Exp. Med. 187, 143–146.
Shi, X., Nuttall, A.L., 2003. Brain Res. 967, 1–10.
Shi, X., Ren, T., Nuttall, A.L., 2002. Hear. Res. 164, 49–58.
Shi, X., Dai, C., Nuttall, A.L., 2003. Hear. Res. 177, 43–52.
Shizuki, K., Ogawa, K., Matsunobu, T., Kanzaki, J., Ogita, K., 2002. Neurosci. Lett. 320, 73–76.
Spicer, S.S., Schulte, B.A., 1996. Hear. Res. 100, 80–100.
Suko, T., Ichimiya, I., Yoshida, K., Suzuki, M., Mogi, G., 2000. Hear. Res. 140, 137–144.
Takemura, K., Komeda, M., Yagi, M., Himeno, C., Izumikawa, M., Doi, T., Kuriyama, H., Miller, J.M., Yamashita, T., 2004. Hear. Res. 196, 58–68.
Takumida, M., Anniko, M., 2001. Acta Oto-Laryngol. 121, 342–345.
Wang, Y., Liberman, M.C., 2002. Hear. Res. 165, 96–102.
Wang, Y., Hirose, K., Liberman, M.C., 2002. J. Assoc. Res. Otolaryngol. 3, 248–268.

Watanabe, K., Inai, S., Jinnouchi, K., Bada, S., Hess, A., Michel, O., Yagi, T., 2002. Anticancer Res. 22, 4081–4085.
Wooten, M.W., 1999. J. Neurosci. Res. 58, 607–611.
Xu, J., Fan, G., Chen, S., Wu, Y., Xu, X.M., Hsu, C.Y., 1998. Brain Res. Mol. Brain Res. 59, 135–142.
Yamane, H., Nakai, Y., Takayama, M., Konishi, K., Iguchi, H., Nakagawa, T., Shibata, S., Kato, A., Sunami, K., Kawakatsu, C., 1995. Acta Oto-Laryngol., Suppl. 519, 87–92.
Yamasoba, T., Harris, C., Shoji, F., Lee, R.J., Nuttall, A.L., Miller, J.M., 1998. Brain Res. 804, 72–78.

WILEY InterScience® DISCOVER SOMETHING GREAT

Journal of Neuroscience Research 83:575–583 (2006)

Proinflammatory Cytokines Expression in Noise-Induced Damaged Cochlea

Masato Fujioka,[1,2] Sho Kanzaki,[1] Hirotaka James Okano,[2,3] Masatsugu Masuda,[1] Kaoru Ogawa,[1] and Hideyuki Okano[2,3]*

[1]Department of Otolaryngology, Head and Neck Surgery, Keio University School of Medicine, Tokyo, Japan
[2]Department of Physiology, Keio University School of Medicine, Tokyo, Japan
[3]Solution Oriented Research for Science and Technology (SORST), Saitama, Japan

Recent studies have showed that inflammatory responses occur in inner ear under various damaging conditions including noise-overstimulation. We evaluated the time-dependent expression of proinflammatory cytokines in noise-exposed rat cochlea. Among several detected cytokines, real-time RT-PCR showed that interleukin-1beta (IL-1β) and interleukin-6 (IL-6) were significantly induced 3 hr after noise exposure, and quickly downregulated to the basal level. Tumor necrosis factor-alpha (TNF-α) was also slightly upregulated immediately after noise exposure. Immunohistochemical analysis showed that IL-6 expression was distinctively induced within the lateral side of the spiral ligament. Sequential expression analysis showed that IL-6 immunoreactivity was initially found in the cytoplasm of lateral wall cells, including Type IV and III fibrocytes, and expanded broader throughout the lateral wall, finally to the stria vascularis. Because of the negative Iba-1 staining, IL-6 expression in the early-phase was not due to macrophage or microglia activation. IL-6 was also detected in spiral ganglion neurons at 12 and 24 hr after noise exposure. Our data demonstrates the production of proinflammatory cytokines, including TNF-α, IL-1β, and IL-6, in early phase of noise overstimulated cochlea. IL-6 expression was observed in the spiral ligament, stria vascularis, and spiral ganglion neurons. These cytokines, produced by the cochlear structure itself in response to noise exposure, may initiate an inflammatory response and have some role in the mechanism of noise-induced cochlear damage.

Key words: cochlea damage; inflammation; cytokines; gene expression; hearing

Overexposure to high intense noise is a well known cause of sensorineural hearing loss, clinically and experimentally. Researchers have focused their attention on the pathology of hair cells in noise-induced hearing loss (NIHL) due to the overstimulation of hair cells. However, several recent studies showed the histopathology of nonsensory cells, including lateral wall fibrocytes and stria cells (Hirose and Liberman, 2003), which suggests that alternative pathophysiology and/or physiological responses to noise over-stimulation may also be involved in NIHL. Interestingly, not only their morphological changes including degenerative processes were seen in these cochlea non-sensory cells: the infiltration of monocytes was also observed by histological evaluation (Hirose et al., 2005), suggesting that an early-phase inflammatory response may be involved in noise over-stimulated damage in cochleae.

Fibroblast is generally known as a key regulator in inflammation, inducing secondary inflammatory responses by producing several cytokines, and closing local inflammation with remodeling; as its disorders lead to excessive inflammation (Buckley et al., 2001; Mor et al., 2005). Cochlear lateral wall fibrocytes are also known to produce inflammatory mediators, as shown by several studies. For example, several in vitro studies have reported that cultured cochlear lateral wall fibrocytes produced IL-6 and other inflammatory agents, including chemoattractants for inflammatory cells, when stimulated by IL-1β or TNF-α (Yoshida et al., 1999; Ichimiya et al., 2000). Concomitantly, experimental inner ear inflammation studies have shown the in vivo production of TNF-α, IL-1β, and IL-6 in cochleae, along with synergic leukocyte infiltration; both of these processes were enhanced by lipopolysaccharide (LPS) intraperitoneal injections (Satoh et al., 2003; Hashimoto et al., 2005). In addition, an in vivo loss of function analysis demonstrated that TNF-α was a deteriorating factor for cochlea inflammation (Satoh et al., 2002). These studies are very important because such molecules are, in general, well known for their potential to induce secondary inflammatory responses, including leukocyte infiltration, scar formation, or gliosis in other injured

Contract grant sponsor: Keio University Grant-in-Aid for Encouragement of Young Medical Scientists; Contract grant sponsor: Japanese Ministry of Education, Culture, Sports, Science and Technology.

*Correspondence to: Hideyuki Okano, Department of Physiology Keio University School of Medicine, 35 Shinanomachi, Shinjuku-ku, Tokyo, 160-8582, Japan. E-mail: hidokano@sc.itc.keio.ac.jp

Received 2 December 2005; Revised 30 November 2005; Accepted 30 November 2005

Published online 20 January 2006 in Wiley InterScience (www.interscience.wiley.com). DOI: 10.1002/jnr.20764

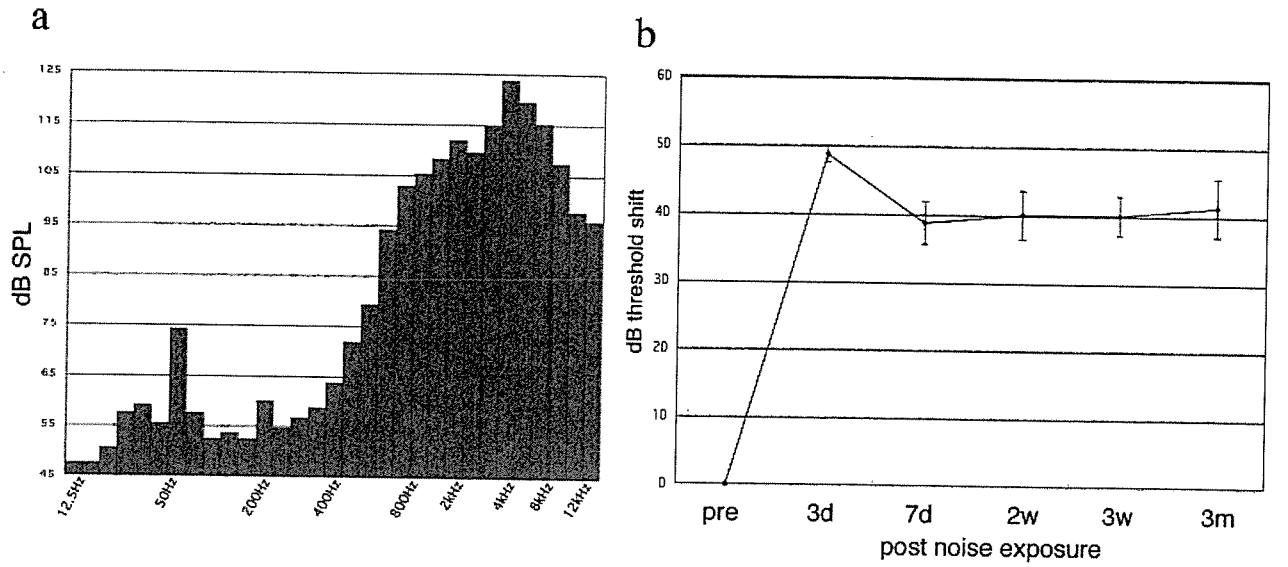

Fig. 1. Noise-induced hearing loss (NIHL) model. Overexposure to large amounts of sound causes hearing loss, but the hearing impairment level depends on the sound intensity, the types of sound, and the susceptibility of the animals. **a:** Sound spectrum used in the experiment, a one-octave-band noise centered at 4 kHz, 124 dB SPL. **b:** Threshold shift we obtained in this experiment ($n = 4$). The hearing level was measured by determining the auditory brain-evoked response (ABR) threshold, and the threshold shift from the pre-noise exposure was defined as the impaired level of hearing. The resulting shift persisted for up to 3 months, with a final shift of 41.3 ± 4.27 dB (mean ± SEM).

organs. These reports indicate the involvement of proinflammatory cytokines in cochlear damage. If the expression of proinflammatory cytokines is demonstrated in cochlea in other models, some physiological or pathophysiological meanings may exist. Evidence of proinflammatory cytokines expression in cochlea has restricted to experimental inflammation or autoimmune diseases. In noise-induced damaged cochlea, the expression of proinflammatory cytokines has not yet been clarified, even though the existence of active inflammatory cells has been reported (Hirose et al., 2005). Considering this background, determining the expression of proinflammatory cytokines under noise-stimulated conditions may help us to understand the early phase of inflammation in NIHL, both physiologically and pathophysiologically. In the present study, we evaluated the expression of cytokines in cochlea using RT-PCR. In addition, we carried out an immunohistochemistry analysis to determine the distribution of IL-6 expression in cochleae after noise exposure.

MATERIALS AND METHODS

Animal Preparation

Four-to-six-week-old male Sprague-Dawley (SD) rats with normal Preyer reflexes were used ($n = 50$). The animals were purchased from Saitama-Experimental Animal Center and were bred in Laboratory Animal Center, School of Medicine, Keio University under SPF conditions. All procedures were approved by the ethics committee of Keio University Union on Laboratory Animal Medicine in accordance with the Guide for the Care and Use of Laboratory Animals (National Institute of Health, Bethesda, MD).

Noise Exposure

In all the experiments, the animals were exposed for 2 hr to octave-band noise (OBN) with a peak at 4 kHz, 124 dBSPL. The noise was generated by an audiometer (AA-67N, RION, Tokyo, Japan) with a masking noise at 4 kHz and was amplified sequentially using two amplifiers: SRP-P150 (SONY, Tokyo, Japan) and D-1405 (FOSTEX, Chesterfield, MO). The animals and speakers were placed in the same box that had been used previously in our laboratory (Shizuki et al., 2002). To deliver the noise stimulation symmetrically in both ears, the animals were placed in the 12-cm diameter, barreled shape cage that was made with metallic mesh, right under the round-shaped speaker. Before the experiments, threshold shift of both ears in each animal were evaluated. No significant difference was observed between left and right ears ($n = 3$, data not shown). The noise conditions at the animals' location were evaluated before the experiments (Fig. 1a).

Auditory Brainstem-Evoked Response

To determine the magnification of the noise-induced hearing loss under the noise conditions in this study, we tested the threshold shift using the click-evoked auditory brainstem-evoked response (ABR). The ABR of the animals ($n = 4$) was determined 3 days before the noise exposure and 3 days, 1, 2, 3, and 4 weeks and 3 months after noise exposure. The ABR measurements were carried out using methods and equipment reported previously (Hoya et al., 2004). Instead of tone-burst stimuli, click stimuli were used in the present

study. The stimuli were composed of a 0.1-msec plus segment, a 0.1-msec minus segment, and alternating polarity outputs. Generally, the ABR waveforms were recorded for 12.8 msec at a sampling rate of 40,000 Hz using 50–5,000 Hz band-pass filter settings, and the waveforms from 256 stimuli at a frequency of 9 Hz were averaged. The ABR waveforms were recorded in 5-dB SPL intervals decreasing from the maximum amplitude until the waveform could no longer be visualized.

Dissection and Sample Preparation

Immediately after 3, 6, 12, or 24 hr or 7, 14, or 28 days after noise exposure, the animals were anesthetized with xylazine (10 mg/g) and ketamine (40 mg/g) and decapitated. The temporal bones were carefully removed from the skull base, and the bulla were opened to expose cochleae. The right cochlea was dissected at the hook using scissors and placed in 750 μl of Trizol Reagent (Invitrogen Corp., Carlsbad, CA) for RNA extraction. The left (or both in several animals) temporal bones were sampled and soaked in 4% paraformaldehyde (PFA) for immunohistochemical analysis (from 0–24 hr post-exposure, $n = 6$;, from 7–28 days post-exposure, $n = 4$; non-exposed control cochlea, $n = 6$). Several right cochleae from 3- or 6-hr post-exposed and non-exposed rats were also sampled for Western blot analysis. The cochlea duct was rapidly dissected using microsurgery. The tissues were then homogenized in ice-cold lysate buffer containing a cocktail of protease inhibitors (Complete, EDTA-free; Roche, Mannheim, Germany), 50 mM of sodium fluoride and 1 mM of sodium orthovanadate. After sonication, the samples were centrifuged at 12,000 rpm for 20 min at 4°C and then stored at −20°C until electrophoresis.

RT-PCR Analysis

Reverse transcriptase reaction with random primers (nonamers) was carried out using a SuperScript III RT-PCR Kit (Invitrogen). The first-strand cDNA was synthesized from 0.5 μg of total RNA. For each PCR experiment, a negative RT control (non-RT RNA) and a negative PCR control (no cDNA template) were also conducted. Second-step RT-PCR was carried out using messageScreen Rat Inflammatory Cytokine Set 2 Multiplex PCR Kits (BioSource International Inc., Camarillo, CA) with 39 cycles of polymerase chain reaction. The thermal cycling conditions of the vendor's protocol for Taq polymerase (Takara Biotechnology Co., Ltd., Otsu, Japan) were followed.

Quantitative real-time RT-PCR reactions were carried out for TNF-α, IL-1β, and IL-6 using Mx3000p (Stratagene, La Jolla, CA). As an internal control, 18S rRNA cDNA was amplified. The TaqMan probes for TNF-α, IL-1β, and IL-6 were all combined with FAM, and those for 18S rRNA were combined with VIC (Applied Biosystems, Foster City, CA). Another fluorescent dye, ROX, was used as a calibrator. The relative expression levels of each cytokine were statistically analyzed using a one-way ANOVA.

Western Blot Analysis

Each sample containing 2.5 μg of protein was subjected to 15% polyacrylamide gel electrophoresis and transferred to a polyvinylidene difluoride membrane. The blots were incubated overnight at 4°C with rabbit anti-IL-6 antibody diluted 1:500 (Sigma, St. Louis, MO), or rabbit anti-IL-6 receptors (IL-6R) antibody (diluted 1:200, Santa Cruz Biotechnology, Santa Cruz, CA). After incubation for 1 hr at room temperature with secondary antibody conjugated with biotin, the blots were incubated with ABC Elite complex (Vectastain ABC Elite Kit; Vector Laboratories Co., Burlingame, CA) and visualized using the ECL Blotting Analysis System (Amersham Bioscience Co., Little Chalfont, UK).

Cryosections and Immunostaining for IL-6

After fixation with 4% PFA, the bony labyrinths were further incubated with Decalcifying Solution A (Plank Rychlo method solution: Wako Pure Chemical Industries, Doshomachi, Osaka, Japan) for 24 hr, dehydrated in a stepwise-manner from 10–30% sucrose, and embedded in Tissue-Tek O.C.T. Compound (Sakura Finetechnical Co., Tokyo, Japan). Series of 6 μm-thick cryosections were then collected onto New Silane II slides (MUTO Pure Chemicals Co., Tokyo, Japan). All of the slides were washed with PBS, incubated in 1.5% hydrogen peroxide for 15 min, rinsed three times in PBS, and incubated in 10% normal goat serum for 1 hr at room temperature and in primary antibodies at 4°C overnight. The primary antibody was the antibody used in the present Western blotting analysis, diluted 1:150. The slides were then incubated in a 1:1,000 dilution of biotinylated secondary antibodies at 37°C for 30 min, washed three times in PBS, then incubated in Elite ABC Kit (Vector Laboratories, Burlingame, CA) for 30 min at room temperature. After a gentle washing in PBS three times, the samples were incubated in diaminobenzidine (DAB) solution (Wako Pure Chemical Industries) for visualization. After washing with PBS, the samples were dehydrated and mounted with cover glasses. The primary antibodies used for the immunofluorescent study were mouse anti-NeuN monoclonal antibody (diluted 1:100, CHEMICON, Temecula, CA) and rabbit anti-IL-6 polyclonal antibody (diluted 1:150). The secondary antibodies were Alexa Fluro (A-11029; Molecular Probes, Eugene, OR) or HRP conjugated antibody (both diluted 1:1,000). The slides were visualized using a TSA-rhodamine visualizing kit (Perkin-Elmer, Boston, MA) according to the manufacture's protocol.

RESULTS

Evaluation of Hearing Impairment Induced by the Noise Exposure

With the noise centered at 4 kHz in a one-octave-wide band of which the peak magnitude was 124 dBSPL (spectrum shown in Fig. 1a.), we produced a noise-induced hearing loss (NIHL) model in the present experiment. The time course of the threshold shift in this model, evaluated using a click-evoked auditory brainstem-evoked response (click ABR), is shown in Figure 1b. The stable threshold shift for up to 3 months suggested that the noise was intense enough to produce a permanent threshold shift (PTS). The final threshold shift level was 41.3 ± 4.27 dB (mean ± SEM) .

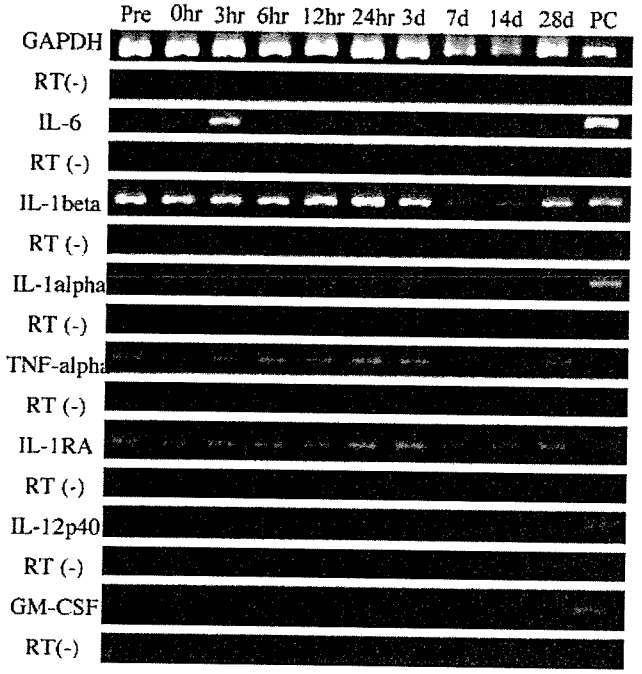

Fig. 2. RT-PCR. Two-step RT-PCR was used to screen for the expression of seven cytokines ($n = 3$). TNF-α, the IL-1 family (IL-1α, β, receptor antagonist), and IL-6, were detected but IL-12 p40 and GM-CSF were not detected. The total RNA quantity in each lane was the same. (PC, positive control; GAPDH, internal control) Note that with unknown reason, the signals at Day 7 and Day 14 of TNF-α, IL-1α, and IL-1β seemed to be low, however, the PCR product of GAPDH at these time-points were also lower than the other time-points.

Transient Upregulation of Proinflammatory Cytokines After Noise Exposure

We carried out a two-step RT-PCR analysis to screen for the expression of cytokines related to inflammation (Fig. 2). Among the seven cytokines that we evaluated, TNF-α, the IL-1 family (IL-1α, β and receptor antagonist). and IL-6 were detected before or after noise exposure. The signals of TNF-α were relatively weak, but detected in a normal state to 28 days after noise exposure. The expressions of IL-1β and IL-1α were detected before and after noise exposure. IL-1RA expression did not change throughout the experiments with or without noise exposure. The expression of IL-6 was detected 0 and 3 hr after noise exposure but then diminished to an undetectable level. IL-12 p40 and GM-CSF expression was not detected.

To assess the precise time-dependent alterations in transcription, we carried out quantitative real-time RT-PCR analyses for TNF-α, IL-1β, and IL-6 using TaqMan probes with 18S rRNA as reference gene. Figure 3 illustrates the expression levels of the RNAs for each cytokine at eight time points after or without noise exposure. Significant IL-1β and IL-6 inductions were detected at 3 hr after exposure ($P < 0.05$, one-way ANOVA). These inductions decreased to the basal level within 24 hr. The same tendency was also observed for TNF-α, whereas no significant differences were detected among the time points.

Western Blot Analysis

We carried out a Western blot analysis to examine IL-6 protein level (Fig. 3d,e). A 27-kDa IL-6 protein was detected as a single band by using an anti-IL-6-specific antibody. Relative upregulation was observed in 3 hr after noise exposure, compared to untreated (i.e., pre-noise) cochleae. After 6 hr, the protein level was significantly upregulated from that for the pre-noise condition. There was no significant difference in the expression of IL-6 receptor (IL-6R) before and after noise exposure (data not shown).

IL-6 Immunostaining After Noise Exposure

To determine which cells produced IL-6, immunohistochemistry for IL-6 was carried out. In pre-noise-exposed cochleae, diffuse weak immunoreactivity was detected in the lateral wall, except for in the stria vascularis. Faintly immunolabeled cells were located in the supra stria region of the lateral wall cells (the area where type V fibrocytes are located) and the spiral prominence (Fig. 4a). At 6 hr after exposure, distinctively immunolabeled cells were observed in the lower part of the cochlea lateral wall cells, including Type III and IV fibrocytes (Fig. 4b). The distribution of IL-6 immunoreactivity was restricted to the cytoplasm of these cells (Fig. 4d,f–h). Among the cochlea turns, a relatively higher immunoreactivity was seen in the apical turn, compared to the basal turn (Fig. 4e). No immunoreactivity was detected without primary antibody incubation (data not shown). Although the IL-6 immunoreactivity was observed in tectorial membrane, we speculate that the staining is background because this region is known to be a high-background area. (Murata et al., 2004; Yamashita et al., 2004).

Figure 5 shows the time-dependent changes in IL-6 immunostaining. Up until 6 hours after noise exposure, the expression pattern became gradually stronger and broader from the lowest part to the higher part of the lateral side of the spiral ligament (Fig. 5a–c). Concomitantly, the IL-6 immunopositive area expanded, from the lateral side toward the medial end of the lateral wall and finally to the damaged stria cells at 12 hr after exposure (Fig. 5b–d).

At 12 and 24 hr after noise exposure, many ganglion cells were immunolabeled for IL-6 in their cytoplasm (Fig. 6d,e), whereas no immunoreactivity was observed within 6 hr (Fig. 6a–c). Diffusely distributed IL-6 immunoreactivity was observed among the ganglion cells (Fig. 6f,g). High-magnification images show the localization of IL-6 and NeuN, a mature neuronal marker. IL-6 immunoreactivity was localized on the surface of some ganglion neurons (Fig. 6h–k,l; arrowheads) and also in the cytoplasm of other neurons (Fig. 6j–l; arrow).

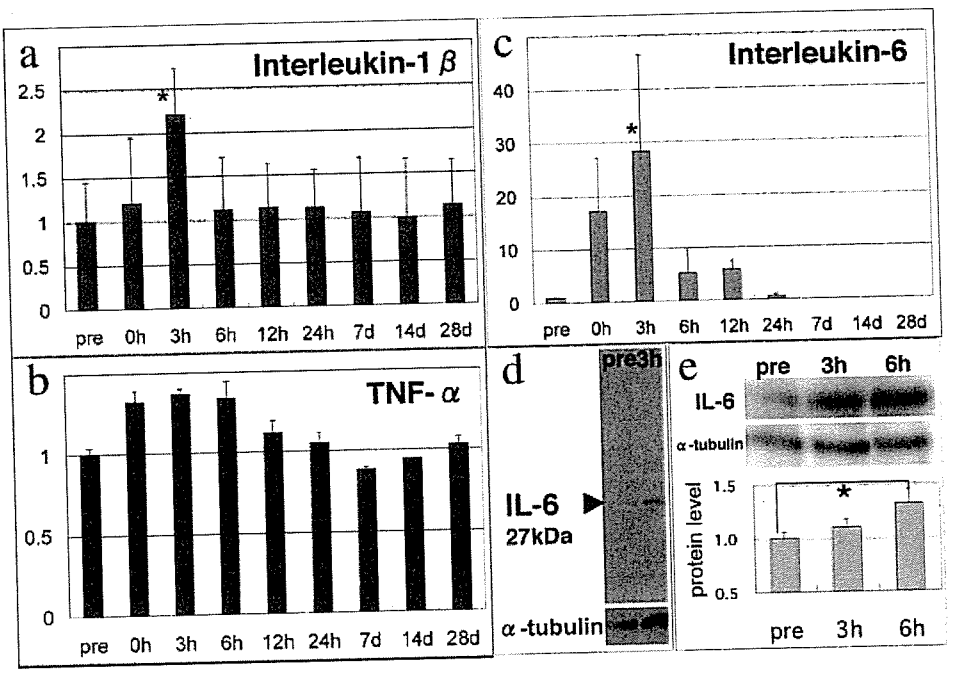

Fig. 3. Quantitative RT-PCR and Western blotting. Quantitative RT-PCR analyses of TNF-α, IL-1β, and IL-6 were carried out using TaqMan probes and 18S rRNA as a reference gene (**a–c**). The amplitude of interleukin-6 RNA expression was the largest of all three cytokines (c). The vertical bar represents the relative ratio of (target gene)/(reference gene). Note that the scales of the vertical bars differ for each target gene. From pre-noise to 24 hr, each $n = 6$; from 7 days to 28 days, each $n = 4$. **d,e:** A whole cochlear Western blotting analysis for IL-6. A single band was detected at the appropriate protein size, demonstrating the high specificity of the IL-6 antibody (d). e: The results of Western blotting for IL-6 at three different time points. A significant difference in IL-6 expression was observed at 6 hr after noise exposure. The vertical bar represents the relative ratio of IL-6 versus α-tubulin (internal control).

DISCUSSION

Proinflammatory cytokines are produced in various organs after tissue damage not only in experimental immune-response models, but also in various types of insults including infection, ischemia, trauma, cryo-ablation, and burns (Berti et al., 2002; Pier et al., 2004), by various types of cells, including residential immune-related cells (such as leukocytes, macrophages, microglia, dendritic cells), neurons and glia in the central nervous system (CNS). We demonstrated that these inflammation-related cytokines were upregulated in noise-induced damaged cochlea and that the time courses of their expressions were very similar to those seen in other traumatized organs. Our data was compatible with the results of several histopathological studies that have pointed out the possibility of inflammatory changes in noise overstimulated cochleae (Hirose et al., 2003, 2005).

In the present study, we demonstrated the induction of IL-6 in lateral wall cells in the early phase of noise-induced cochlear trauma. IL-6 RNA and protein inductions were detected at 3 and 6 hr after noise exposure, respectively. Furthermore, the cytoplasmic expression of IL-6 protein in lateral wall cells appeared in the lower and lateral areas of the spiral ligaments, suggesting that IL-6 protein was newly produced by translation between 3 and 6 hr after noise exposure. Fibrocytes in cochlear lateral wall were anatomically and histologically classified into four (or five; depending on the researchers) subtypes, each of which has particular function (Spicer and Schulte, 1991, 1996). The IL-6 immunoreactive cells in the lower part of lateral wall are interpreted as Type IV and III fibrocytes. Interestingly, we also observed the expression and relative induction of IL-1β and TNF-α before IL-6 RNA expression after noise exposure. Previous reports showed that cochlea lateral wall fibrocytes produce IL-6 when stimulated by IL-1β and TNF-α in vitro (Ichimiya et al., 2003). Based on the findings of this and former reports, we speculate that IL-6 may be produced in vivo in cochleae, initially by Type IV and III fibrocytes via the synergetic stimulation of IL-1β and TNF-α. Activated microglia and monocytes have been known to produce cytokines in other damaged organs, including brain injuries (Allan and Rothwell, 2001; Lo et al., 2003). Our data clearly demonstrated that the IL-6-expressing cells were not colocalized with Iba-1-positive cells in this area (Iba-1 is a specific marker for activated macrophages or monocytes). Therefore, we concluded that the IL-6 expression observed in this study was not by activated immune-related cells, like homing macrophages or microglia.

In addition, a double-labeling study showed the presence of IL-6 expression in NeuN-positive neurons of the spiral ganglion at 12–24 hr after noise exposure, although not all of the NeuN-positive neurons expressed IL-6. IL-6 induction in the spiral ganglion neurons might

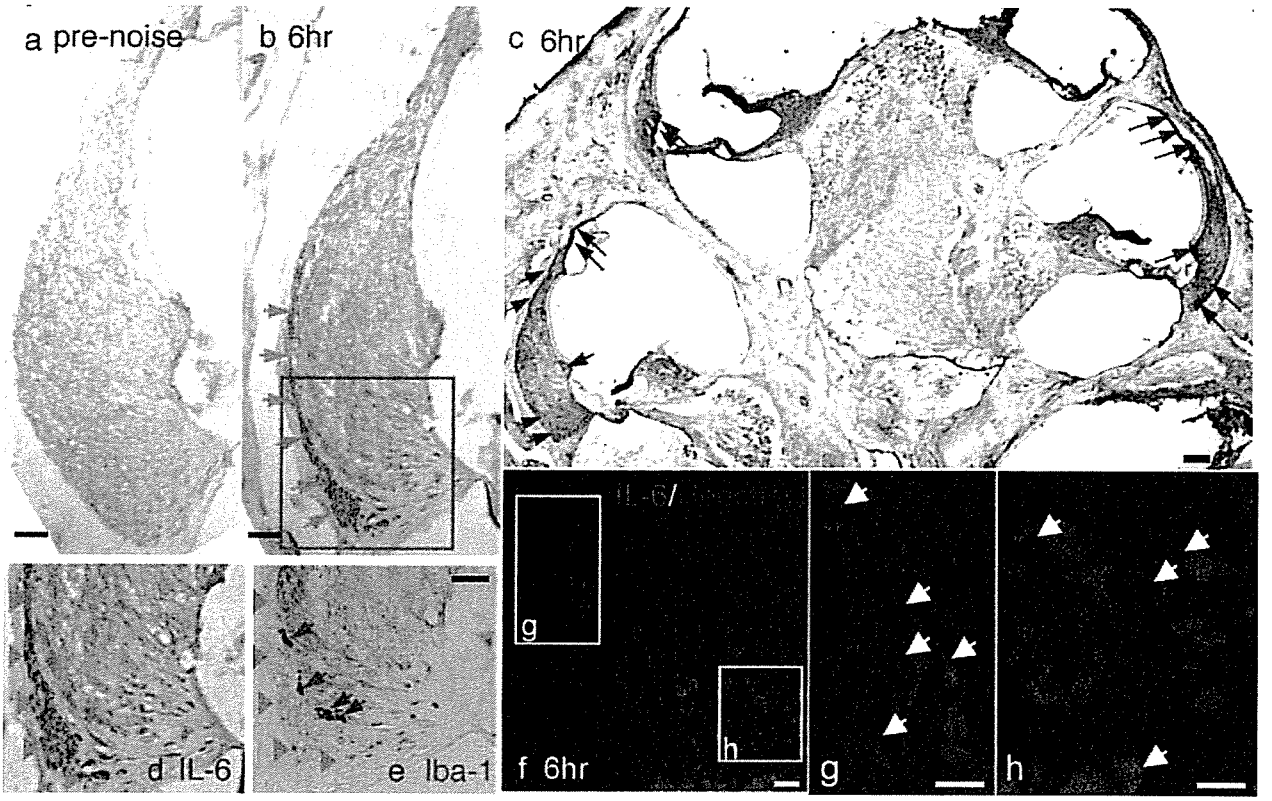

Fig. 4. Immunostaining of IL-6. Immunohistochemistry of interleukin-6 in the noise-exposed cochleae. At 6 hr after exposure, prominent IL-6 immunoreactivity was found in the lateral side of the spiral ligament (orange arrows in **b**, blue arrows in **c**, orange arrowheads in **d**). IL-6 immunoreactivity was distributed in the cytoplasm of the lateral wall cells. Morphologically, these cells include Type III and IV fibrocytes (arrows in b–d,**g,h**). d,**e**: Serial sections. IL-6 expression (orange arrows in d) was not colocalized with Iba-1 (red arrows in e), an activated macrophage or microglia marker. Note that IL-6 was not expressed in the stria vascularis at this time point. **a**: Control cochlea b–h: 6 hr after noise exposure. a–d: IL-6, e: Iba-1, **f**–h: red, IL-6; blue, Hoechst 33432. Scale bars = a–e, 50 μm; f–I, 20 μm.

reflect the second peak of IL-6 RNA production observed 12 and 24 hr after noise exposure. In the CNS, mature neurons produce IL-6 in response to various cellular stresses, including ischemia and excitotoxic stress (Suzuki et al., 1999; Acarin et al., 2000; Block et al., 2000). Our data suggest IL-6 production in the spiral ganglion neurons may also due to cellular stresses, including noise overstimulation, because overstimulation of hair cells induces a secondary degeneration in spiral ganglion (Lim, 1976; Webster and Webster, 1981).

IL-6 is an intercellular signaling molecule via paracrine or autocrine manners. One of the roles of IL-6 is its anti-oxidative stress effect by upregulating several anti-apoptotic genes, including bcl-family, or cell survival signals (Lin et al., 2001). Another role is regulating inflammation including immune responses. Knock-out mice study has shown that, in cryo-ablated brain, the loss of IL-6 production suppresses macrophage recruitment and decreases local inflammation, but increases apoptosis in injured cells (Morganti-Kossmann et al., 2002).

The localization of diffuse IL-6 immunoreactivity in damaged cochleae should be crucial. In the lateral wall, IL-6 immunoreactivity was observed initially in and around Type IV fibrocytes; then expanded diffusely and broadly toward the stria cells. In the spiral ganglion, IL-6 immunoreactivity was seen not only in the cytoplasm, but also on the cell surface of neurons. Lateral wall fibrocytes and stria cells are crucially important for generating endocochlear potential (EP) and ion transportation, both of which are indispensable for auditory hair cells to generate action potential in response to sound stimuli (Spicer and Schulte, 1996; Crouch et al., 1997; Flagella et al., 1999; Kikuchi et al., 2000). These cells are susceptible to noise-induced overstimulation, and among them, Type IV fibrocytes are the most susceptible cells, which undergo apoptotic degeneration and never repopulate (Hirose and Liberman, 2003). Taking all these data together, our data suggest the possibility that Type IV fibrocytes might be the initiator of the local inflammatory response against the stress in cochlea.

Several published reports suggested that the involvement of IL-1 family and TNF-α in damaged cochleae (Komeda et al., 1999; Satoh et al., 2002; Wang et al., 2003). Although the mechanism and function of these

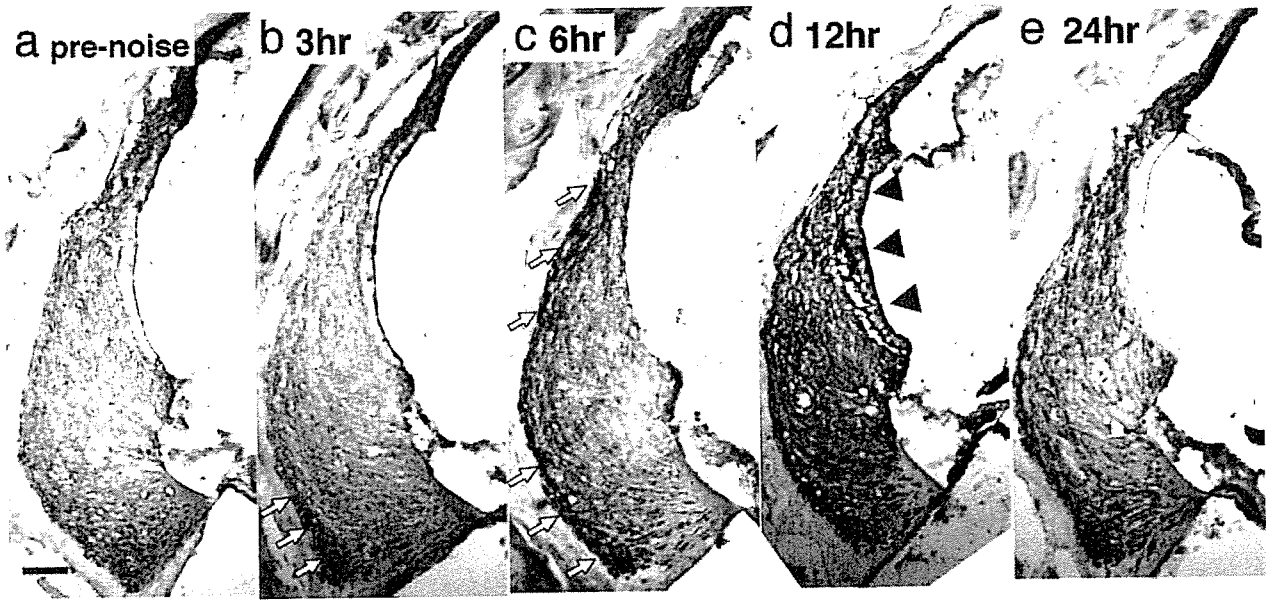

Fig. 5. Time-dependent expression of IL-6 in the lateral wall of the cochlear basal turn. At 3 hr after exposure, moderately immunolabeled cells were found in the lowest region of the lateral wall, where Type IV fibrocytes are located (**b**). At 6 hr after noise exposure, IL-6 immunoreactive cells had increased markedly, expanding from the lowest region to the higher region of the lateral side of the wall (white arrows) (**c**). From 3–12 hr after exposure, IL-6 immunoreactive area broadened from lateral to medial and finally extended to the swollen, vacuolizing stria cells (**d**, arrowheads). The diffuse IL-6-positive area had mostly disappeared at 24 hr after noise exposure (**e**). In the spiral prominence and supra-stria fibrocytes, weak immunoreactivity was detected from pre-noise to 24 hr after noise exposure. **a:** control cochlea; b–e: 3, 6, 12, 24 hr after noise exposure. Scale bar = 50 μm.

cytokines in NIHL are still obscure, suppression of infiltration of inflammatory cells into cochleae by inhibiting TNF-α signal has been demonstrated to reduce hearing loss in experimental inner ear inflammation model (Satoh et al., 2002; Wang et al., 2003). Our present data led us to believe that inhibition of IL-6 signal in the acute phase of NIHL would also be a therapeutic strategy. Therapeutic interventions against acute inflammation by targeting IL-6 have been tried, but two loss-of-function analyses in examining CNS injuries reported opposite results: the blockage of IL-6 signaling in spinal cord injury ameliorated functional recovery (Okada et al., 2004), whereas the same treatment aggravated cerebral damage in an experimental cerebral ischemia model (Yamashita et al., 2005). These results indicate that the expression of IL-6 acts as a double-edged sword in the CNS, and the function of IL-6 is context-dependent, presumably depending largely on the type of cells and the type of stresses. The biological meaning of IL-6 expression in noise-induced hearing loss remains unclear. Although it might be a self-protecting mechanism against exposure to large amounts of sounds, excessive expression would worsen long-term cochlear function. In the latter case, the expression of IL-6 in the early phase could be a therapeutic target of artificial manipulations, similar to the strategies that have been used for spinal cord injuries or rheumatoid arthritis (Ito et al., 2004; Nishimoto et al., 2005; Yokota et al., 2005). Thus, a loss-of-function analysis is critically important and should be attempted in NIHL model in the near future.

This is the first study demonstrating the induction of proinflammatory cytokines in noise-exposed cochleae. Clinically, appropriate doses of steroid-based therapy have been chosen for many years as a favorable option for preventing long-term cochlear function in patients with acoustic trauma. The effects of steroid-based treatments against noise-induced hearing loss might be due to an anti-inflammatory reaction, suppressing excessive inflammation. However, large dose of steroids harmed long-term cochlear function by some experimental studies (Karlidag et al., 2002; Takemura et al., 2004). This variable outcome of steroid treatment might be explained by the actions of multifunctional proinflammatory cytokines, like IL-6 whose expression is actually suppressed by steroid treatment in lateral wall fibrocytes in vitro (Maeda et al., 2005). Recent drug-design technology has enabled us to suppress cytokine-mediated inflammation with fewer side effects using non-steroid anti-inflammatory agents, specific inhibitors of each cytokine. For example, in patients with rheumatoid arthritis (RA) or inflammatory bowel disease, the blockage of IL-6 by specific humanized neutralizing antibodies has been clinically used with promising effects (Nishimoto et al., 2004). Our present study suggests the possibility of therapeutic strategies tar-